iScience

CellPress
OPEN ACCESS

Article

Using brain cell-type-specific protein interactomes to interpret neurodevelopmental genetic signals in schizophrenia

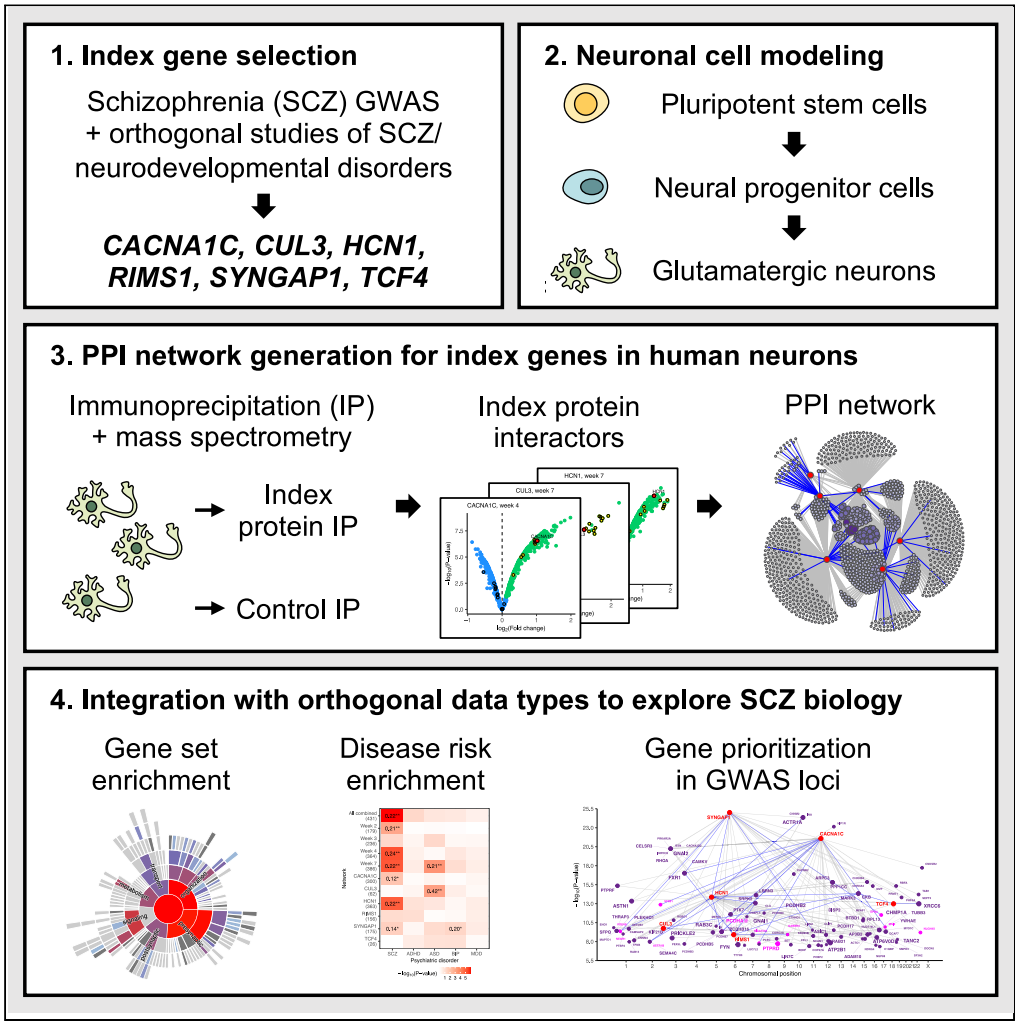

Yu-Han H. Hsu, Greta Pintacuda, Ruize Liu, ..., Hailiang Huang, Kevin C. Eggan, Kasper Lage

kevin.eggan@bmrn.com (K.C.E.)
lage.kasper@mgh.harvard.edu (K.L.)

Highlights

Protein-protein interaction network for 6 schizophrenia risk genes in human neurons

The network is enriched for common variant risk of schizophrenia across ancestries

The network complements fine-mapping and eQTL data to prioritize genes in GWAS loci

Convergence of common and rare variant risks in the HCN1 sub-network

Hsu et al., iScience 26, 106701
May 19, 2023
https://doi.org/10.1016/j.isci.2023.106701

iScience

CellPress
OPEN ACCESS

Article

Using brain cell-type-specific protein interactomes to interpret neurodevelopmental genetic signals in schizophrenia

Yu-Han H. Hsu,[1,2,3,11] Greta Pintacuda,[1,2,4,11] Ruize Liu,[1,5,11] Eugeniu Nacu,[1,4,11] April Kim,[1,6,11] Kalliopi Tsafou,[1] Natalie Petrossian,[1] William Crotty,[1] Jung Min Suh,[1] Jackson Riseman,[1] Jacqueline M. Martin,[1] Julia C. Biagini,[1] Daya Mena,[1] Joshua K.T. Ching,[1] Edyta Malolepsza,[7] Taibo Li,[1] Tarjinder Singh,[1,5] Tian Ge,[1,8] Shawn B. Egri,[9] Benjamin Tanenbaum,[9] Caroline R. Stanclift,[9] Annie M. Apffel,[9] Schizophrenia Working Group of the Psychiatric Genomics Consortium, Stanley Global Asia Initiatives, Steven A. Carr,[9] Monica Schenone,[9] Jake Jaffe,[9] Nadine Fornelos,[1,2,3] Hailiang Huang,[1,5] Kevin C. Eggan,[1,4,*] and Kasper Lage[1,2,3,10,12,*]

SUMMARY

Genetics have nominated many schizophrenia risk genes and identified convergent signals between schizophrenia and neurodevelopmental disorders. However, functional interpretation of the nominated genes in the relevant brain cell types is often lacking. We executed interaction proteomics for six schizophrenia risk genes that have also been implicated in neurodevelopment in human induced cortical neurons. The resulting protein network is enriched for common variant risk of schizophrenia in Europeans and East Asians, is down-regulated in layer 5/6 cortical neurons of individuals affected by schizophrenia, and can complement fine-mapping and eQTL data to prioritize additional genes in GWAS loci. A sub-network centered on HCN1 is enriched for common variant risk and contains proteins (HCN4 and AKAP11) enriched for rare protein-truncating mutations in individuals with schizophrenia and bipolar disorder. Our findings showcase brain cell-type-specific interactomes as an organizing framework to facilitate interpretation of genetic and transcriptomic data in schizophrenia and its related disorders.

INTRODUCTION

Schizophrenia is a debilitating psychiatric disorder occurring in ~0.3% of the global population with severe repercussions for patients, families, and society.[1,2] The last years have seen great advances in mapping the genetic architecture of schizophrenia, identifying hundreds of common and rare variants that confer risk for the disorder across diverse populations.[3–10] These studies also revealed overlapping genetic signals between schizophrenia, autism spectrum disorders (ASD), and severe developmental disorders (DD), supporting the importance of neurodevelopmental processes in the pathophysiology of schizophrenia.[9–11] However, although the identified schizophrenia risk genes provide a good entry point for systematic studies of the disorder and its related conditions, their molecular functions and interactions in the brain remain poorly understood, hindering the development of effective treatments and therapeutics.[12,13]

In parallel, analyses of *postmortem* brains from individuals with schizophrenia and integration of genetic and transcriptomic data from human and mouse brains have converged on cortical excitatory neurons as a key biological conduit of genetically encoded risk.[14–17] This suggests that systematic mapping of schizophrenia risk genes onto protein-protein interaction (PPI) networks in this cell type could reveal mechanisms and pathways underlying schizophrenia.[18,19] A seminal study showed that adding extrinsic neuronal patterning to pluripotent stem cells (PSCs) overexpressing *NGN2* generates glutamatergic induced neurons (iNs) that behave like cortical excitatory neurons at the molecular, morphological, and functional levels.[20,21] Here, we leveraged this protocol to perform interaction proteomics for six schizophrenia risk genes that have also been implicated in neurodevelopment in a neuronal cell model. By integrating the resulting PPI networks with orthogonal datasets, we showed that our approach creates a unique

Continued

[1]Stanley Center for Psychiatric Research, Broad Institute of MIT and Harvard, Cambridge, MA 02142, USA

[2]Novo Nordisk Foundation Center for Genomic Mechanisms of Disease, Broad Institute of MIT and Harvard, Cambridge, MA 02142, USA

[3]Department of Surgery, Massachusetts General Hospital, Boston, MA 02114, USA

[4]Harvard Stem Cell Institute and Department of Stem Cell and Regenerative Biology, Harvard University, Cambridge, MA 02138, USA

[5]Analytic and Translational Genetics Unit, Department of Medicine, Massachusetts General Hospital, Boston, MA 02114, USA

[6]Department of Computer Science, Johns Hopkins University, Baltimore, MD 21218, USA

[7]Genomics Platform, Broad Institute of MIT and Harvard, Cambridge, MA 02142, USA

[8]Psychiatric and Neurodevelopmental Genetics Unit, Center for Genomic Medicine, Massachusetts General Hospital, Boston, MA 02114, USA

[9]Proteomics Platform, Broad Institute of MIT and Harvard, Cambridge, MA 02142, USA

[10]Institute of Biological Psychiatry, Mental Health Centre Sct. Hans, Mental Health Services Copenhagen, 4000 Roskilde, Denmark

opportunity to investigate the roles of schizophrenia risk genes and their associated pathways in a brain cell-type-specific context.

RESULTS

Prioritization of schizophrenia index genes with shared neurodevelopmental signals

To identify schizophrenia risk genes as the basis of our interactome experiments we designed and executed a three-step procedure (Figure 1A and Table S1). First, we identified 445 genes (Set 1) in previously reported genome-wide significant loci from the Psychiatric Genomics Consortium (PGC) genome-wide association study[3] (GWAS; phase 2). Second, we filtered this set to 37 genes (Set 2) within single protein-coding gene loci, excluding other genes in loci with more ambiguous association signals. Third, we integrated data from orthogonal studies (e.g., high-density genotyping, exome sequencing, and earlier targeted studies of individual genes; STAR Methods and Table S1) to identify a subset of 10 genes (Set 3) supported by multiple independent lines of evidence. Importantly, we used orthogonal evidence from rare variant studies of ASD/DD to prioritize schizophrenia risk genes that have also been implicated in neurodevelopmental conditions. We additionally included *SYNGAP1* in the major histocompatibility complex (MHC) region in all three sets because of strong orthogonal evidence for its involvement in schizophrenia and neurodevelopmental disorders.

Genes implicated in schizophrenia are under strong genetic selection and have elevated expression in the frontal cortex.[9] Therefore, to assess the enrichment of schizophrenia risk genes in Sets 1–3, we compared their gnomAD[22] pLI scores (i.e., the probability of being loss-of-function intolerant, where genes under strong selection have higher pLI scores) and BrainSpan[23] expression to schizophrenia risk genes from the recent Schizophrenia Exome Sequencing Meta-Analysis (SCHEMA) study.[9] In terms of pLI scores, Sets 1–3 all have increasingly higher scores compared to other genes in the genome (one-tailed KS test p = 1.1e-3, 1.7e-3, and 1.3e-5 for Sets 1–3, respectively; Figure 1B and Table S2). Set 3 scores are significantly higher than that of Set 2 (one-tailed KS test p = 5.8e-4), which in turn are higher than that of Set 1 (one-tailed KS test p = 0.019). Furthermore, Set 3 is under the same degree of constraint as the exome-wide significant (FDR < 3.7e-3) SCHEMA genes (two-tailed KS test p = 0.23). In terms of gene expression, Set 1 mirrors the expression profile of random genes during frontal cortical development up until adulthood; Set 2 has a postnatal expression profile that resembles SCHEMA genes with FDR of 0.25–0.5; and Set 3 has a postnatal expression profile that strongly mirrors the exome-wide significant SCHEMA genes (Figure 1C and Table S3). Although the lower prenatal expression of Set 3 compared to the SCHEMA genes may be reflecting different aspects of schizophrenia-related biology captured by common versus rare variants, respectively (Data S4), the pLI scores and postnatal expression patterns generally support our three-step approach to gene selection based on refining GWAS data and indicate that Set 3 is enriched for bona fide schizophrenia risk genes. We proceeded to use Set 3 as the starting point of our experiments and refer to these 11 genes and their encoded proteins as 'index genes' and 'index proteins', respectively.

Interaction proteomics of schizophrenia index proteins in excitatory iNs

To study the expression patterns of the index proteins throughout iN maturation, we tested 58 commercially available antibodies and identified 31 with competency to detect the 11 index proteins (Table S4). We differentiated iPSCs into neural progenitor cells (NPCs; day 3) and iNs (weeks 2–7) and confirmed protein expression of CACNA1C, CACNB2, CSMD1, CUL3, GRIN2A, HCN1, RIMS1, SYNGAP1, and TCF4 in neuron lysates by western blot (Figures 1D and S1). SATB2 and ZNF804A lacked detectable neuronal expression or high-quality reagents and were excluded from further experiments. When comparing index protein expression between iNs, non-neuronal cells, and mouse cortex, CACNA1C, CSMD1, GRIN2A, HCN1, RIMS1, and SYNGAP1 displayed a neuron-specific expression profile.

Next, we tested 42 antibodies for their ability to immunoprecipitate (IP) the index proteins (Table S4) and were able to IP seven index proteins (CACNA1C, CACNB2, CUL3, HCN1, RIMS1, SYNGAP1, TCF4) in ~seven billion iNs for subsequent mass spectrometry (MS) analyses. In total, we carried out 23 IP-MS experiments at five neuronal differentiation time points. We performed quality control (QC) and analyzed each experiment using Genoppi,[24] calculating the $\log_2$ fold change (FC) and corresponding statistical significance for each protein identified in the index protein IPs compared to the controls, and then defining proteins with $\log_2$ FC > 0 and FDR ≤ 0.1 as the significant interactors of the index protein. We disregarded four IP experiments that did not meet our QC criteria (i.e., the $\log_2$ FC correlation between replicates was < 0.5 or the index protein itself was not enriched at FDR ≤ 0.1). The remaining 19 high-quality IPs of CACNA1C, CUL3, HCN1,

[11]These authors contributed equally

[12]Lead contact

*Correspondence: kevin.eggan@bmrn.com (K.C.E.), lage.kasper@mgh.harvard.edu (K.L.)

https://doi.org/10.1016/j.isci.2023.106701

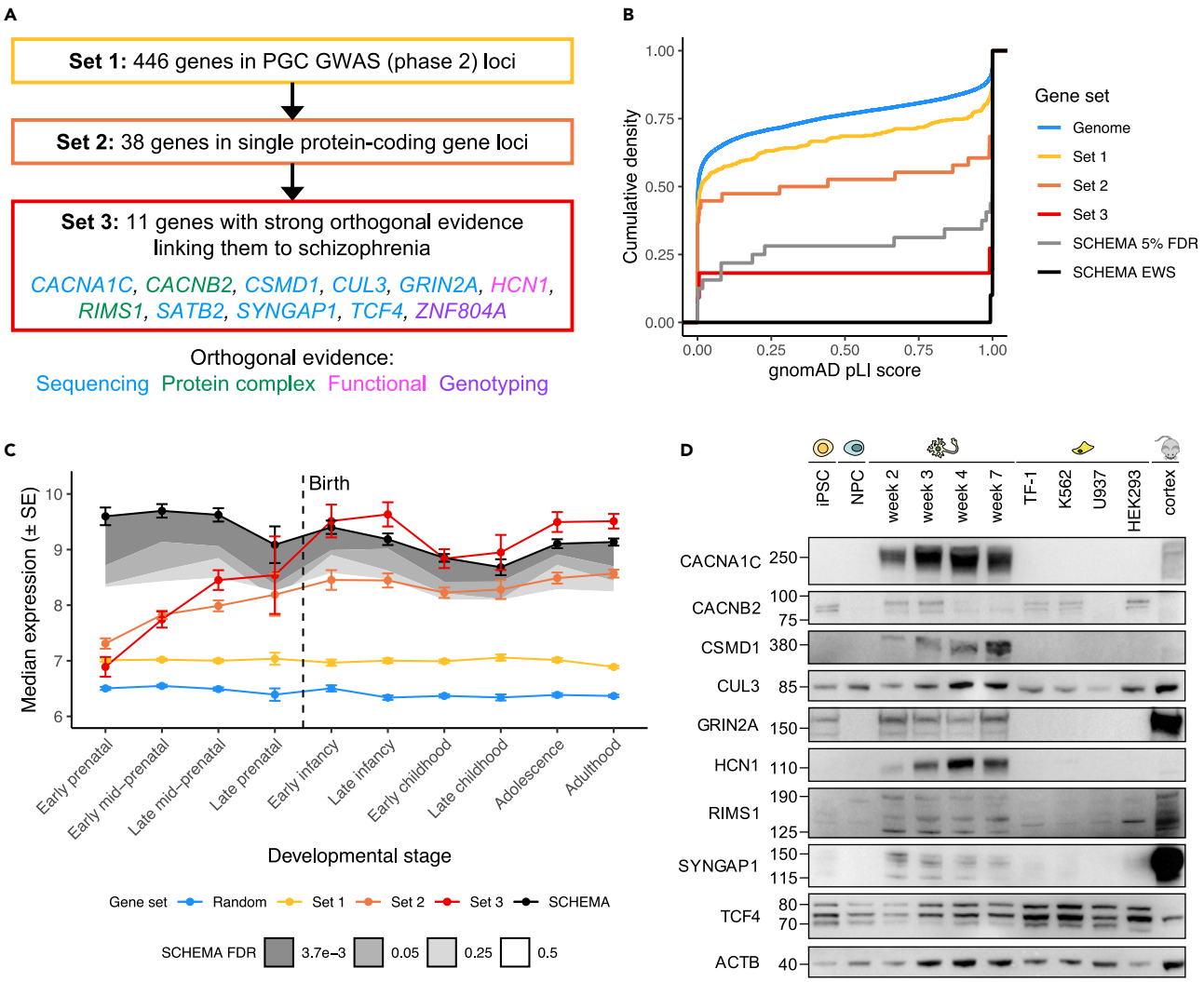

Figure 1. Selection of schizophrenia index genes and proteins for interactome experiments

(A) Three-step procedure to identify Sets 1–3 by refining schizophrenia GWAS [PGC phase 2] data, where Set 3 was defined as 'index genes' and used as the basis for downstream experiments. Set 3 genes are color-coded based on the type of orthogonal evidence supporting their involvement in neuropsychiatric or neurodevelopmental phenotypes.

(B) Cumulative density of gnomAD pLI scores for different gene sets. 'Genome' indicates genes in the pLI dataset [excluding Sets 1–3]; 'Sets 1–3' indicate genes in Sets 1–3 with available pLI scores; 'SCHEMA 5% FDR' and 'SCHEMA EWS' indicate genes with FDR < 0.05 or 3.7e-3 [exome-wide significance] in the SCHEMA exome sequencing analysis, respectively.

(C) Frontal cortex RNA expression of gene sets across ten developmental stages. Median expression and standard error [SE] of each gene set were derived from the BrainSpan exon microarray dataset. 'Random' indicates genes randomly sampled from the BrainSpan dataset; 'Sets 1–3' indicate genes in Sets 1–3 with available BrainSpan data; 'SCHEMA' indicates exome-wide significant genes from SCHEMA. Shaded regions indicate median expression of genes with FDR < 3.7e-3 [exome-wide significance], 0.05, 0.25, or 0.5 in SCHEMA with darker gray indicating greater significance.

(D) Western blot analysis of index proteins in iPSCs, NPCs [at day 3 of differentiation], iNs [at weeks 2–7 of differentiation], three cancer cell lines [TF-1, K562, U937], HEK293 cells, and mouse cortex. SATB2 and ZNF804A are excluded from this panel due to lack of detectable expression in iNs. See also Figure S1, Data S4, and Tables S1, S2, S3, and S4.

RIMS1, SYNGAP1, and TCF4 had a median replicate $\log_2$ FC correlation of 0.87, with the six index proteins enriched at a median FDR of 8.2e-4 (Figures 2A, 2B, S2A, S2B; Tables S5 and S6). In addition, we performed experimental and computational analyses to confirm that, despite using an inclusive FC cutoff (i.e., $\log_2$ FC > 0) to define index protein interactors in the IPs, the interactors showed no obvious quality differences across a range of different FCs (Data S5).

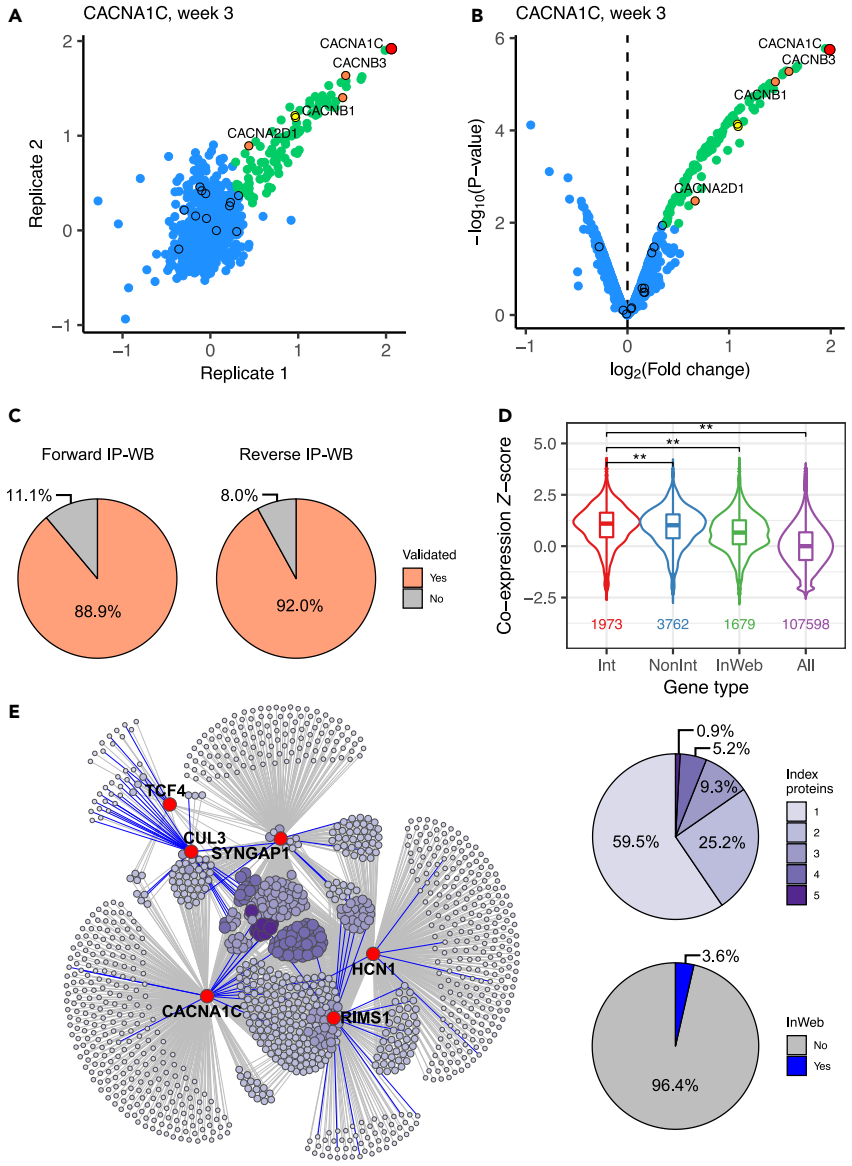

Figure 2. Cell-type-specific protein interactomes in cortical human neurons

(A) Scatter plot showing $\log_2$ FC correlation between replicate 1 [x-axis] and replicate 2 [y-axis] of an IP of CACNA1C at week 3 of neuron differentiation [Pearson's $r = 0.74$].

(B) Volcano plot showing $\log_2$ FC [x-axis] and $-\log_{10}$ p-value [y-axis] of the CACNA1C IP from (A). For (A) and (B), the index protein [CACNA1C] is shown in red, significant interactors [$\log_2$ FC > 0 and FDR $\leq$ 0.1] in green, and non-interactors [i.e., other detected proteins] in blue. Known InWeb interactors are indicated by black border circles, with the subset that are significant in the IP highlighted in yellow [overlap p = 1.8e-2]. Calcium channel components [alpha, beta, and alpha2delta subunits] are in orange.

(C) Replication rates of a subset of interactions tested in forward or reverse IPs followed by western blotting [IP-WB].

(D) Pairwise co-expression Z-scores between index genes and their interactors [Int], non-interactors [NonInt], known InWeb interactors [InWeb], and all protein-coding genes [All] derived from a spatial transcriptomic dataset in human dorsolateral prefrontal cortex. Boxes and whiskers in violin plots indicate the interquartile range [IQR] and 1.5x IQR, respectively. Double asterisks indicate $p < 0.05/6$ [adjusting for six pairwise comparisons] as calculated by two-tailed Wilcoxon rank-sum tests. Number of gene pairs plotted for each gene type is indicated toward the bottom.

(E) The combined interaction network of six index proteins resulting from 19 individual IPs. Index proteins and their interactors are indicated as red and purple nodes, respectively. Size and color of the interactor nodes scale with the

Figure 2. *Continued*
number of index proteins linked to each interactor, with larger and darker nodes representing more recurrent interactors [distribution shown in upper right pie chart]. Edges represent protein interactions with colors indicating whether each interaction is known in InWeb [blue] or potentially novel [gray; distribution shown in lower right pie chart]. See also Figures S2 and S7, Data S5 and S6, and Tables S4, S5, S6, S7, S8, S9, and S10.

The PPI data contain newly reported and reproducible interactions

Importantly, our experimental design was purposely aimed at generating inclusive PPI datasets that encompass non-stoichiometric interactions, rather than restricting to direct interactions and core molecular complexes (Data S6). In previous work, we have established that the replication rate of interactions identified using a similar IP-MS approach is 70–90%.[24] In the current study, we were able to recapitulate these estimates using a two-pronged approach (Figures 2C and S3–S5, and Table S7). First, we performed western blots of 45 interactors for the six index proteins on repetition of the index protein IPs and validated 40 of the interactors (88.9% replication rate). In parallel, we performed reverse IPs using a panel of interactors as baits, and successfully detected the original index proteins in 23 out of 25 reverse IPs that showed bait enrichment (92.0% replication rate). The ~90% replication rates are in general agreement with the 10% FDR cutoff we applied to identify significant interactions.

Besides replicating a subset of the index protein interactors, we also used published datasets to assess the biological validity of our IP-MS data. First, ten of the 19 IPs are further supported by the observation that they are enriched for known protein interactors derived from the InWeb database[25] (Table S5). As an example, in a CACNA1C IP performed in iNs at week 3 of differentiation, the significant interactors are enriched for known CACNA1C interactors in InWeb ($p = 1.8e-2$), including all known L-type calcium channel subunits: the extracellular CACNA2D1 and the intracellular CACNB1 and CACNB3[26] (Figures 2A and 2B). On the other hand, >94% of the interactors are not found in InWeb nor in an IP of CACNA1C executed in mouse heart tissue with the same antibody.[27] This example illustrates that our neuron-derived PPI data capture both known and novel biology as expected, given that existing PPI datasets were mostly generated in non-neuronal context using different experimental methods (Data S6).

We also used brain co-expression data to systematically benchmark all index protein interactors in our data, reasoning that on average, transcripts of interacting proteins would be more likely to co-localize across tissues, cell types, and developmental time points (STAR Methods). Indeed, we observed that the interactors usually have higher co-expression with the index proteins compared to the 'non-interactors' (i.e., non-significant proteins detected in IP-MS), known interactors in InWeb, and all protein-coding genes in a spatial transcriptomic dataset derived from human dorsolateral prefrontal cortex[28] (Figure 2D). Similar trends were also observed in other expression datasets from human or mouse brains[29,30] (Figure S2C). This not only indicates that the interactions we identified in *in vitro* neurons represent biology found in complex brain tissues, but further suggests that they may be more enriched for gene relationships in the brain compared to proteins generally expressed in neurons (represented by the non-interactors) or interactions found in non-neuronal context (represented by the InWeb interactors). In summary, the experimental replications, InWeb overlap, and brain co-expression results all support the quality, reproducibility, and biological relevance of the interactome data we have generated for the schizophrenia index proteins in human iNs.

The combined PPI networks for six schizophrenia index proteins

When we compared multiple IPs of the same index protein across time points during neuronal maturation and between cell lines (for CACNA1C, HCN1, and SYNGAP1), we observed significant agreement in terms of the $\log_2$ FC correlation of all detected proteins (median correlation = 0.75; Figures S6A and S6C–S6E). When we clustered the IPs based on the percentage of overlap between significant interactors, we found that IPs from the earlier versus the later time points tend to fall into separate clusters, agreeing with known characteristics of maturing neurons generated using the NGN2-based protocol[21] (Figures S6B and S6D–S6F and Table S8). However, we also observed relatively high percentages of overlap that are statistically significant across all time points (median percentage = 72%). Overall, these results indicate that our IPs from different time points capture a large proportion of overlapping biology, which is not unexpected given that differentiating iPSCs start to express neuronal markers soon after forcing NGN2 overexpression. Based on these observations, we decided to explore the combined PPI network of each index protein across time points in downstream analyses.

We merged data from the 19 individual IPs to create nine additional consolidated datasets (Table S9). These datasets represent the combined PPI network of a single index protein across multiple experiments or time points (i.e., CACNA1C, HCN1, RIMS1, and SYNGAP1), the combined network of multiple index proteins at one time point (i.e., week 2, 3, 4, and 7), and the combined network of all six index proteins across all time points (i.e., 'all combined'). The all combined network contains 1,238 interactors of the six index proteins and, like the CACNA1C IP highlighted above, >96% of the interactions in this network are potentially novel interactions not found in InWeb (Figure 2E and Table S5). Genes encoding these interactors have relatively high expression in the frontal cortex throughout brain development similar to schizophrenia risk genes reaching 5% FDR in SCHEMA (Figure S7A, Table S3, and Data S4). SynGO[31] gene set analysis also found the network to be enriched for genes involved in various biological processes in the synapse (Figure S7B and Table S10). Overall, we successfully mapped the neuronal protein interactomes of six proteins that are transmembrane (CACNA1C, HCN1), cytosolic (CUL3, SYNGAP1), and involved in multiple neuronal signaling processes (RIMS1, SYNGAP1, TCF4). The resulting PPI networks include a high percentage of newly reported interactions and span many areas of the cell biology of cortical excitatory neurons.

The PPI networks are enriched for genetic risks of schizophrenia, ASD, and DD

To test the networks for association to schizophrenia, we assessed the enrichment of common variant risk across the networks using PGC GWAS data containing schizophrenia cases and controls of European (EUR) or East Asian (EAS) ancestry.[3,8] For these and all further network enrichment analyses, we created a more conservative version of the combined networks by excluding proteins that showed up as non-interactors in any of the source IPs (see 'stringent interactors' in Table S9). In total, we performed genetic analyses for 11 interaction networks, including the nine combined networks and two individual IP networks for CUL3 and TCF4. Importantly, our analyses were conditional on the non-interactors detected in our IP experiments, meaning that we tested whether interactors in the different networks are enriched for genetic risk compared to other iN-expressed proteins. If so, this would suggest that our networks are relevant to schizophrenia over and above the background proteome of the neuronal cell model.

Using MAGMA,[32] we found that many of the PPI networks are indeed enriched for schizophrenia risk when conditioned on other iN-expressed proteins. Notably, the enrichment is generally consistent across EUR and EAS ancestries (Figure 3A and Table S11). At a Bonferroni-corrected threshold ($p < 0.05/22$, adjusting for 11 networks and two ancestries), the week 4 network in both EUR and EAS ancestries, as well as the all combined, week 2, week 7, and HCN1 networks in EAS showed significant enrichment. In the cross-ancestry meta-analysis, the all combined, week 2, week 4, week 7, and HCN1 networks were all significant at the same Bonferroni-corrected threshold. In parallel, we further validated these findings using a genetic risk score (GRS) enrichment analysis method that estimates the genetic risk on holdout samples not included in GWAS and therefore is less sensitive to outliers (STAR Methods). Most results were replicated, including the enrichment signals for the all combined, week 4, and HCN1 networks in both ancestries and their meta-analysis (Figure S8B and Table S11).

To further explore whether the genetic risk enrichment we observed in the PPI networks is specific to schizophrenia, we repeated the same analyses using GWAS data of other psychiatric disorders, including attention deficit hyperactivity disorder[33] (ADHD), ASD,[34] bipolar disorder[35] (BIP), and major depressive disorder[36] (MDD), as well as height[37,38] as a control trait (Figures 3A, 3B, S8A, and S8B, and Table S11). Across these phenotypes, we only observed robust enrichment for ASD in the CUL3 network and the week 7 network which contains IP data of CUL3 and SYNGAP1, both of which have been previously linked to ASD.[39,40] The networks that showed the most robust enrichment for schizophrenia (i.e., the all combined, week 4, and HCN1 networks) did not demonstrate enrichment for the other phenotypes.

Besides analyzing data from common variants, we also tested whether the PPI networks are enriched for rare variant risks of schizophrenia,[9] ASD,[40] and DD,[41] as well as for high gnomAD pLI scores (Figure S8C and Table S11). At a Bonferroni-corrected threshold ($p < 0.05/11$, adjusting for 11 networks), we found the CUL3 network to be enriched for DD genes, which agrees with the previously implicated role of CUL3 in developmental delay.[39,42] In addition, the week 4 and RIMS1 networks are significantly enriched for genes with high pLI scores, indicating that some members of these networks are likely intolerant to loss-of-function mutations and may be involved in essential cell functions.

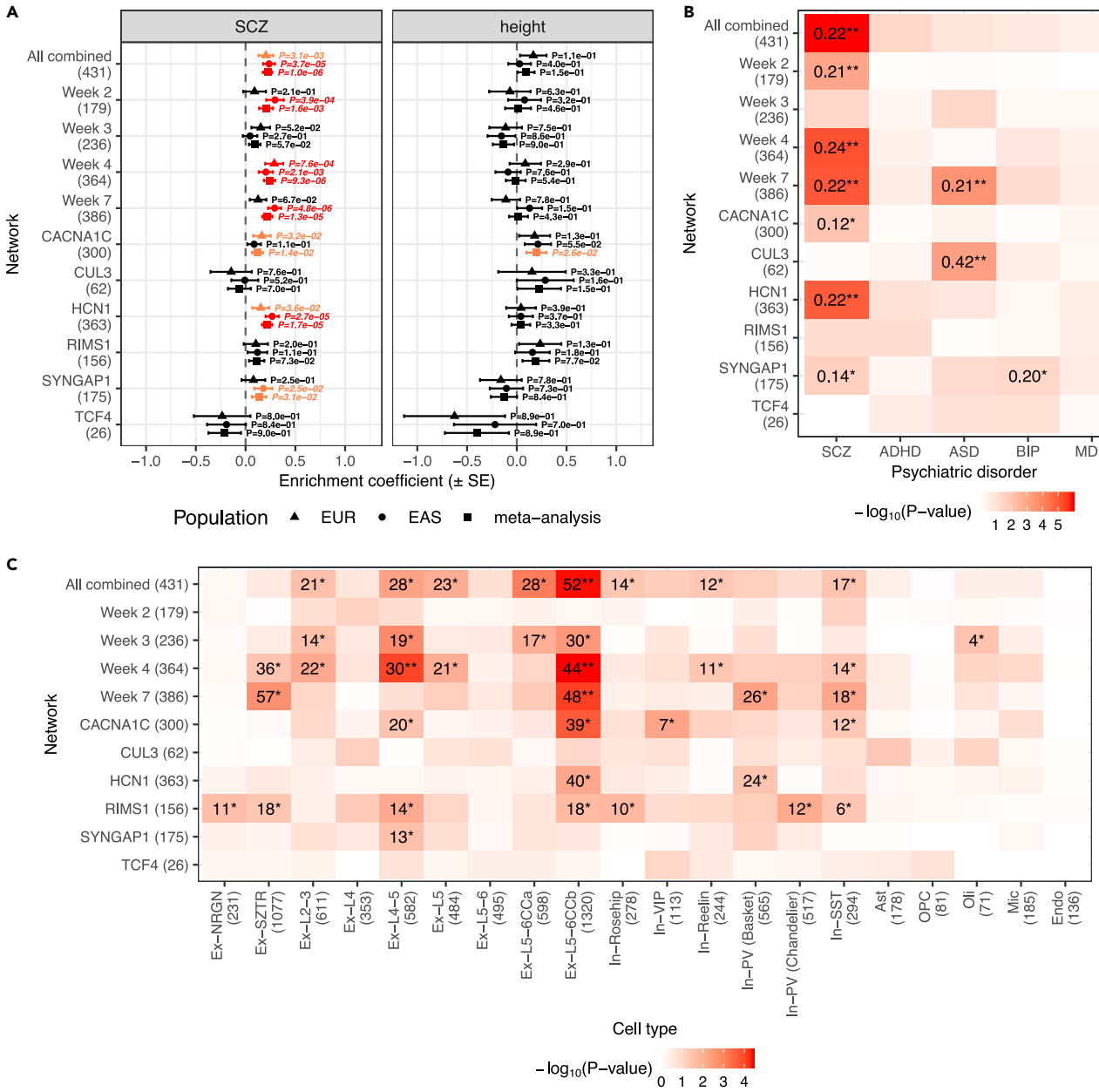

Figure 3. Enrichment of common variant risks and transcriptional perturbations in the index protein interactomes

Networks tested are the combined network of all IPs [All combined], the combined networks at each time point [Week 2 to Week 7], the combined networks for CACNA1C, HCN1, RIMS1, and SYNGAP1, and the individual IP networks for CUL3 and TCF4; the number of genes in each network is shown in parentheses on the y-axes.

(A) Common variant enrichment of schizophrenia [SCZ] or height in Europeans [EUR], East Asians [EAS], or their meta-analysis. Enrichment coefficients, standard errors [SE], and p-values were calculated using MAGMA. $p < 0.05$ or $p < 0.05/22$ [adjusting for 11 networks and two ancestries] results are highlighted in orange or red, respectively.

(B) Common variant enrichment of SCZ, attention deficit hyperactivity disorder [ADHD], autism spectrum disorders [ASD], bipolar disorder [BIP], or major depressive disorder [MDD] calculated using MAGMA. Cross-ancestry meta-analysis results are shown for SCZ; EUR ancestry results are shown for other disorders. Enrichment coefficients reaching $p < 0.05$ or $p < 0.05/22$ significance are shown in the heatmap followed by single or double asterisks, respectively.

(C) Enrichment of cell-type-specific differentially expressed genes [DEGs] in the prefrontal cortex of schizophrenia patients compared to controls; the number of DEGs in each cell type is shown in parentheses on the x-axis. p-values were calculated using one-tailed hypergeometric tests. Gene counts in overlaps reaching $p < 0.05$ or $p < 0.05/220$ [adjusting for 11 networks and 20 cell types] significance are shown in the heatmap followed by single or double asterisks, respectively. See also Figures S8 and S9, Tables S11 and S12.

Overall, these genetic analysis results indicate that most of the PPI network genes are specifically concentrating common variant risk of schizophrenia, whereas several sub-networks are also enriched for common or rare variant risks of ASD/DD, highlighting the shared biology between these disorders.

The PPI networks implicate layer 5/6 cortical excitatory neurons in schizophrenia

Next, we explored whether the PPI networks are enriched for brain-layer-specific transcriptional perturbations observed in patients with schizophrenia. We analyzed data from a recent single-cell RNA sequencing study,[17] which identified differentially expressed genes (DEGs) in individuals with schizophrenia versus controls in 20 annotated cell types in the prefrontal cortex. Many of our networks had nominally significant ($p < 0.05$) overlaps with the cell-type-specific DEGs in neuronal cell types, which include both upper and deep layer excitatory neurons and inhibitory interneurons (Figure 3C and Table S12). A population of layer 5/6 cortico-cortical projection neurons ('Ex-L5-6CCb') showed the most robust enrichment, reaching Bonferroni significance ($p < 0.05/220$, adjusting for 11 networks and 20 cell types) for the all combined, week 4, and week 7 networks. Subsequently, we separately analyzed the up- and down-regulated DEGs in this cell-type, showing that the enrichment signals are strongly driven by the down-regulated DEGs (Figure S9 and Table S12). As DEGs in 'Ex-L5-6CCb' were also found to be enriched for genes implicated by schizophrenia GWAS,[10] there is an intriguing convergence between our results and findings in patients that converge on deep layer cortical excitatory neurons as a key cell type for studying cellular networks involved in schizophrenia.

The PPI data complement orthogonal approaches to prioritize risk genes from GWAS loci

Functionally interpreting GWAS data to identify causal genes based on genome-wide significant SNPs is a major challenge in the field of genetics. Because our analyses indicate that the combined PPI network of all IPs is genetically and transcriptionally relevant in schizophrenia, we used the network to prioritize additional schizophrenia risk genes in GWAS loci. We created a 'social Manhattan plot' by integrating our PPI data with the most recent PGC schizophrenia GWAS[10] (phase 3), highlighting observed interactions between the index proteins and other proteins (locus proteins, hereafter) encoded by genes in the 287 genome-wide significant loci (Figure 4A and Table S13). In total, we identified 123 locus proteins in 74 loci that are linked to ≥ 1 index protein in the social Manhattan plot. We further intersected these locus proteins with those prioritized by fine-mapping (FINEMAP) or eQTL co-localization (summary-based Mendelian randomization, SMR) analysis, pinpointing nine proteins that were also prioritized by FINEMAP (ACTR1B, EPN2, GABBR2, KIAA1549, MSI2, NEGR1, NLGN4X, PDE4B, PTPRD) and three proteins that were also prioritized by SMR (PCDHA2, PCDHA8, SF3B1). In addition, our network was able to nominate candidate genes in 44 distinct loci that lack prioritization results from FINEMAP or SMR analysis.

To further compare our network prioritization approach to FINEMAP or SMR, we looked at the pLI score distributions and BrainSpan expression profiles of several gene sets, including all genes in the GWAS loci (PGC3), genes prioritized by our network (Network), FINEMAP, or SMR, and genes prioritized by both our network and either FINEMAP or SMR (Overlap). The Network and FINEMAP genes both have significantly higher pLI scores compared to all PGC3 genes (one-tailed KS test $p = 7.9e\text{-}6$ and $2.0e\text{-}4$, respectively) and genes in the same loci as the prioritized genes (one-tailed KS test $p = 1.4e\text{-}6$ and $1.1e\text{-}4$, respectively; Figure 4B and Table S2). In contrast, the SMR genes did not show such enrichment. The Overlap genes have even higher pLI scores that are comparable to the SCHEMA genes with FDR < 0.05 (two-tailed KS test $p = 0.36$), although the differences between the Overlap genes and other genes in the Network, FINEMAP, or SMR supersets are not statistically significant. When looking at gene expression throughout frontal cortical development, the Network, FINEMAP, SMR, and Overlap genes all have elevated expression compared to all PGC3 genes. In particular, the Network and Overlap genes have higher expression than the FINEMAP and SMR genes; their postnatal expression profiles are close to that of the high-confidence SCHEMA genes (Figure 4C and Table S3).

We also compared the Network genes to other PGC3 genes encoding iN-expressed proteins (i.e., non-interactors in Table S9) and observed that these two gene sets have comparable pLI scores and BrainSpan expression (Tables S2 and S3). These results indicate that the proteome of cultured neurons may contribute to the pLI score and expression enrichment we observed for the Network genes. However, by first showing that our PPI network is significantly enriched for schizophrenia genetic risk and transcriptional perturbations compared to the non-interactors, and then showing that the network genes in GWAS loci have higher pLI scores and frontal cortical expression throughout development compared to other genes in the loci, we

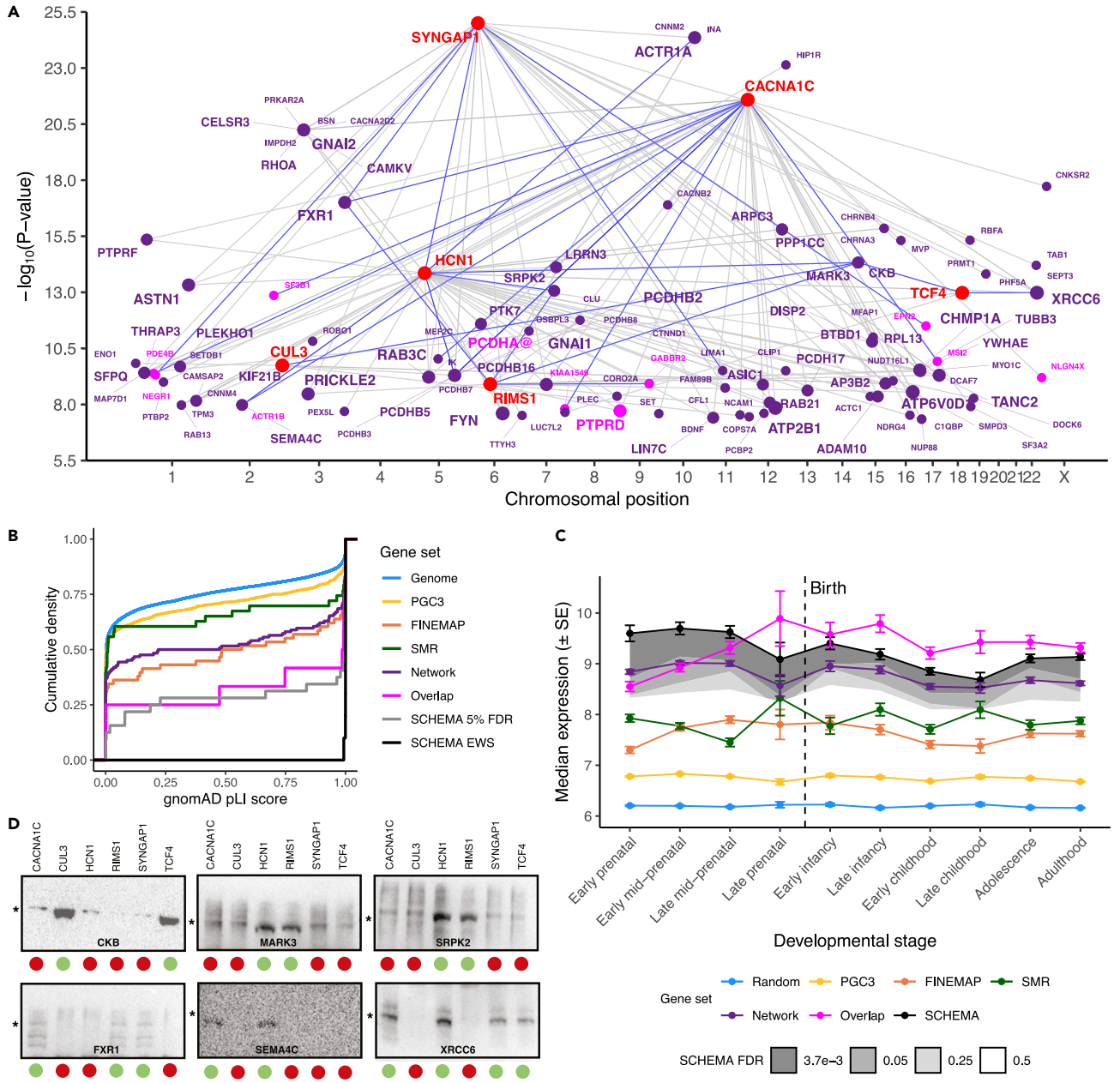

Figure 4. Prioritizing genes in schizophrenia GWAS loci using brain cell-type-specific interactome data

(A) Social Manhattan plot of genes encoding the index proteins [red] and their interactors [purple] in genome-wide significant loci in PGC schizophrenia GWAS [phase 3]. Size of the interactor nodes and their labels scale with the number of index genes linked to each interactor; those that were also prioritized by FINEMAP or SMR analysis are highlighted in magenta. Gray lines indicate observed protein-protein interactions in our data; interactions that have been replicated by IP-WB are highlighted in blue.

(B) Cumulative density of gnomAD pLI scores for different gene sets. 'Genome' indicates genes in the pLI dataset [excluding PGC3 genes]; 'PGC3' indicates genes in PGC GWAS [phase 3] loci; 'FINEMAP', 'SMR', and 'Network' indicate PGC3 genes prioritized by FINEMAP, SMR, or our interactome data, respectively; 'Overlap' indicates genes overlapping between Network and FINEMAP or SMR; 'SCHEMA 5% FDR' and 'SCHEMA EWS' indicate genes with FDR < 0.05 or 3.7e-3 [exome-wide significance] in SCHEMA, respectively.

(C) Frontal cortex RNA expression of gene sets across ten developmental stages. Median expression and standard error [SE] of each gene set were derived from the BrainSpan exon microarray dataset. 'Random' indicates genes randomly sampled from the BrainSpan dataset; 'PGC3', 'FINEMAP', 'SMR', 'Network', and 'Overlap' indicate gene sets as described in (B); 'SCHEMA' indicates exome-wide significant genes from SCHEMA. Shaded regions indicate median expression of genes with FDR < 3.7e-3 [exome-wide significance], 0.05, 0.25, or 0.5 in SCHEMA with darker gray indicating greater significance.

(D) Western blot analysis on independent IPs of index proteins [named on the top] to detect the presence of selected locus proteins [named on the side of each gel]. Green and red circles at the bottom represented whether the tested interaction was significant or non-significant by IP-MS, respectively. Each lane represents 10% of the IP material analyzed by IP-MS. L = ladder. Molecular weights are in KDa. See also Figure S10 and Table S13.

demonstrate how our interactome data can complement orthogonal methods such as fine-mapping and eQTL co-localization analyses to nominate schizophrenia risk genes from GWAS data.

Finally, to illustrate that many of the locus proteins we prioritized could be reproducible interactors of the index proteins, we repeated the index protein IPs and performed western blotting to detect selected interactors; or vice versa, we executed reverse IPs for the interactors followed by western blotting to detect the index proteins. In total, we replicated 25 interactions for 18 unique locus proteins using forward or reverse IPs, including eight proteins that were also prioritized by FINEMAP or SMR, as well as an interaction between two of the index proteins, HCN1 and SYNGAP1 (Figures 4A, S3, and S5, and Table S7). We also performed western blots for several locus proteins on all six index protein IPs in parallel, showing that their detection patterns agree with their significant interactions with distinct index proteins in IP-MS (Figures 4D and S10). These results support the reproducibility of the PPI data and the observed convergence between the index protein interactomes. Follow-up investigation on the prioritized locus proteins can be informative for determining whether their corresponding genes are true schizophrenia risk genes responsible for the genetic signals observed in GWAS.

DISCUSSION

We brought together advances in genetics, neuronal cell modeling, interaction proteomics, and integrative analytical approaches to study cell-type-specific pathway relationships of schizophrenia risk genes in human excitatory neurons. Although previous studies have used PPI data to interpret genetic signals in complex disorders,[18,19] few leveraged neuronal cell models to generate PPI networks in a human cellular context that are important for neuropsychiatric disorders. We showed that the iN-derived PPI networks consist of many newly reported, reproducible (~90% replication rate by western blot) interactions that capture gene relationships found in the human brain, illustrating the potential for biological pathway discovery based on neuron-specific PPI data.

We performed genetic enrichment analyses to validate the relevance of our PPI networks to schizophrenia and related disorders. Strikingly, the all combined network and several sub-networks are enriched for common variant risk of schizophrenia across different populations (Europeans and East Asians) and analytical methods (MAGMA and the GRS method), indicating that the PPI data will be a rich substrate for follow-up investigation of universal molecular mechanisms of schizophrenia. In contrast, we did not observe enrichment for rare variant schizophrenia risk in the networks. Repeating the analysis using larger rare variant datasets in the future may allow us to determine whether this is due to biological differences between common versus rare variants of schizophrenia or because of power limitations in the current data.[9] When we tested for genetic risk enrichment of several other disorders, we found a few networks to be enriched for common or rare variant risks of ASD/DD. This is expected given our choice to prioritize schizophrenia index genes using orthogonal evidence for ASD/DD and agrees with the neurodevelopmental model of schizophrenia.[11] However, the all combined PPI network did not show enrichment for ASD/DD or other disorders that have strong genetic correlations with schizophrenia (e.g., BIP). The lack of enrichment may be because of sample size and power differences between the genetic datasets. Alternatively, it may be because the schizophrenia index genes are not all relevant to the other disorders (e.g., among the index genes, only *CACNA1C* is in genome-wide significant loci of the BIP GWAS).

We also demonstrated how our PPI data can prioritize candidate genes from schizophrenia GWAS data, which is a main bottleneck in post-GWAS analysis.[43] Although statistical fine-mapping can pinpoint the likely causal variants within GWAS loci, it is difficult to generate actionable biological hypotheses based on fine-mapped SNPs.[44] Hence, functional genomics and data types such as eQTLs have been used to complement fine-mapping by providing biological context and identifying SNP-associated genes. A lesson that emerged from these gene prioritization approaches is the importance of using tissue- and cell-type-specific data to dissect genetic signals in a disease-relevant context.[45] However, there is still an underrepresentation of data derived from highly specialized cell types that are difficult to culture in the lab. Furthermore, recent analysis revealed a limited overlap between GWAS signals and eQTLs, indicating a need for orthogonal approaches that do not rely on transcriptomic data.[46] Our study provides a brain cell-type-specific, protein-centric dataset that could address some of these limitations. We used a 'guilt-by-association' approach to prioritize GWAS genes that interact with the high-confidence schizophrenia index genes at the protein level, thereby linking them to interactions, mechanisms, and pathways that can be investigated in a neuronal context. It is exciting that, with a PPI network anchored by just six

index genes, we already obtained promising gene prioritization results that are both complementary to and distinct from fine-mapping and eQTL co-localization, which were performed using genome-scale datasets. This suggests that cell-type-specific PPI data may become increasingly useful and powerful for gene prioritization with increase in scale (e.g., data from additional index genes) and scope (e.g., data from different disease-relevant cell types).

In our analyses, the HCN1 network emerged as a promising lead for follow-up investigation. This network is enriched for schizophrenia common variant risk in both Europeans and East Asians, suggesting that perturbed signaling through the hyperpolarization-activated cyclic nucleotide-gated potassium channel,[47] a heterotetrameric complex consisting of HCN1-4, could play a role in schizophrenia. Two HCN1 interactor genes, *HCN4* and *AKAP11*, are also enriched for schizophrenia-associated protein-truncating variants (PTVs) in SCHEMA (FDR = 4.2e-3 and 1.3e-2, respectively). In a meta-analysis of schizophrenia and bipolar disorder cases,[48] *AKAP11* further emerged as an exome-wide significant (p = 2.8e-9) gene enriched for ultra-rare PTVs. The roles of PTVs in disease are commonly linked to decreased gene function and expression. Indeed, the HCN1 network is suggestively enriched for down-regulated DEGs in layer 5/6 cortico-cortical projection neurons ('Ex-L5-6CCb') of individuals with schizophrenia (Figure S9), supporting the hypothesis that members of the network may be involved in schizophrenia through loss-of-function or decreased expression. Together, these findings implicate a network involved in neuronal potassium signaling in schizophrenia, which also contains drug targets that can be explored in follow-up studies (Figure S11 and Table S14).

Another intriguing finding from our results is the recurrent interaction between CACNA1C and C4A (observed in four out of five CACNA1C IP-MS experiments; Table S6), suggesting that the L-type calcium channel may be a functional binding site of the complement cascade in synaptic pruning of the developing prefrontal cortex. This interaction is consistent with the emerging evidence that complement-mediated modulation of synapse stability or function contributes to risk for schizophrenia.[49,50] We were unable to identify suitable immunoreagents to perform follow-up IP of C4A (Table S4), likely because of its complex post-translational modifications. However, we also identified C3, another component of the complement cascade, as an interactor of CACNA1C in one of the CACNA1C IPs (Table S6). This interaction could be a perhaps better vantage point into the functional characterization of the interplay between synaptic biology and complement cascade, because it is more stable and therefore amenable to biochemical studies.

Limitations of the study

We acknowledge several limitations that should be considered when interpreting the results of our study. First, all IPs were performed in a salt/detergent environment optimized to identify both stable interactions (e.g., between members of core protein complexes) and more transient interactions. Although both may be biologically relevant to schizophrenia, we are unable to discriminate between them with our current IP-MS approach. Second, MS analyses of the IPs were associated with known technical biases, including incomplete coverage and underrepresentation of lowly expressed or highly hydrophobic proteins.[51,52] Therefore, the IP-MS datasets generated in this study do not represent a saturated interactome for each index protein in iNs. Third, although independent IPs and reverse IPs followed by western blotting estimated a ~90% replication rate in our PPI data, these assays shared some of the biases of IP-MS. Technologies such as multichannel microscopy,[53] super-resolution microscopy,[54] and cryo-EM[55] could provide orthogonal validation of the identified interactions.

Finally, our PPI networks were generated from IPs of six index proteins in excitatory neurons, thus they do not represent a complete interactome of all schizophrenia risk genes across different brain cell types. As large-scale rare variant association studies of schizophrenia (e.g., SCHEMA) were not yet available at the conception of our study, we chose to prioritize the common variant schizophrenia index genes using orthogonal rare variant evidence of ASD/DD. Consequently, our findings may be biased toward shared biology between schizophrenia and neurodevelopmental conditions, instead of biology involved more exclusively in schizophrenia. Furthermore, although our neuronal cell model mimics cortical excitatory neurons in the human brain, it may not capture molecular interactions that are influenced by interplay with other cell types (e.g., astrocytes) or only present in later developmental stages (e.g., adolescence). Despite these caveats, our genetic enrichment analyses indicate that the generated PPI networks are indeed capturing schizophrenia-relevant biology. In the future, applying our approach to a wider set of index genes and cell types implicated across the spectrum of schizophrenia and related neurodevelopmental

conditions may allow us to further dissect the convergent versus divergent pathways underlying these conditions in the human brain.

Conclusions

In this study, we leveraged human iPSC-derived excitatory neurons to build PPI networks for six schizophrenia risk genes and integrated the networks with orthogonal data types. Going forward, with larger genetic datasets to identify disease risk genes, wider availability of IP-competent immunoreagents, and the ability to create stem cell models of other brain cell types at the scale required for systematic proteomic experiments, we expect that the approach described here can be applied to uncover additional insights into the biology of schizophrenia and provide rich orthogonal information that is not captured by other approaches such as GWAS, exome sequencing, single-cell RNA sequencing, and whole-proteome analyses. More generally, our study presents an organizing framework to study complex brain disorders and contributes to laying the foundation for a new functional genomic approach in psychiatry. In fact, we have applied the same framework to study ASD-associated genes prioritized by exome sequencing,[56] showing that it can empower interpretation of data from both common and rare variant genetics across two different groups of disorders of the human brain.

STAR★METHODS

Detailed methods are provided in the online version of this paper and include the following:

- KEY RESOURCES TABLE
- RESOURCE AVAILABILITY
  - Lead contact
  - Materials availability
  - Data and code availability
- EXPERIMENTAL MODEL AND SUBJECT DETAILS
  - Cell lines
  - Mouse cortex sample
- METHOD DETAILS
  - iN differentiation
  - Western blotting
  - Immunoprecipitations
  - Immunoprecipitations using V5 epitope tagged TCF4
  - Mass spectrometry
- QUANTIFICATION AND STATISTICAL ANALYSIS
  - Refining geneticdata to identify index genes
  - pLI score enrichment analysis
  - BrainSpan expression profiles
  - IP-MS data analysis
  - Co-expression analysis
  - Consolidating IP-MS datasets into interaction networks
  - SynGO gene set analysis
  - Common variant enrichment analysis using MAGMA
  - Common variant enrichment analysis using the GRS method
  - Rare variant enrichment analysis
  - Transcriptional perturbation enrichment analysis
  - Social Manhattan plot
  - HCN1 network drug target query

SUPPLEMENTAL INFORMATION

Supplemental information can be found online at https://doi.org/10.1016/j.isci.2023.106701.

ACKNOWLEDGMENTS

We thank Carole Manneville, Matthias Mueller, Katie Worringer, and Ajamete Kaykas at Novartis for sharing the hDFn cell line; Ellen Beauchamp, Andrew Guirguis, Rebecca Gorelov, and Zuzana Tothova for sharing cancer cell lines; Karl Clauser for managing and uploading the proteomics data; and Steve

Hyman, Mark Daly, and Ben Neale for insightful scientific discussions. This work was supported by grants from the Stanley Center for Psychiatric Research, the US National Institute of Mental Health (R01 MH109903 and U01 MH121499), the Simons Foundation Autism Research Initiative (awards 515064 and 735604), the Lundbeck Foundation (R223-2016-721 and R350-2020-963), the Novo Nordisk Foundation (NNF21SA0072102), the Augustinus Foundation, the Knud Højgaard Foundation, the Reinholdt W. Jorck og Hustrus Foundation, the US National Institute of Diabetes and Digestive and Kidney Diseases (U01 DK078616 and T32 DK110919), and a Broad Next10 grant.

AUTHOR CONTRIBUTIONS

G.P., E.N., N.P., W.C., J.M.S., J.R., J.M.M., J.C.B., and D.M. carried out tissue culture, tested antibodies for WB/IP experiments and ran WBs. E.N., N.P., W.C., J.M.S., and B.T. executed IP experiments. S.B.E., B.T., C.R.S., A.M.A., M.S. and J.J. ran MS experiments and analysis. S.A.C. supervised the MS experiments. A.K. and E.M. analyzed and consolidated IP-MS data. Y.H.H., K.T. and T.L. consolidated IP-MS data and ran BrainSpan analysis. R.L. performed common variant enrichment analyses. J.K.T.C. performed comparisons of IP-MS data. Y.H.H. performed the rest of the analyses. T.S., T.G., and H.H. designed genetic risk enrichment analyses. N.F. supervised and managed the study. K.C.E. and K.L. designed and supervised the study. K.L. initiated and led the study. Y.H.H., G.P., R.L., E.N., K.T., N.F., H.H., K.C.E. and K.L. wrote the manuscript with input from co-authors.

DECLARATION OF INTERESTS

K.C.E. is a co-founder of Q-State Biosciences, Quralis, and Enclear, and currently employed at BioMarin Pharmaceutical. Other authors declare no competing interests.

INCLUSION AND DIVERSITY

One or more of the authors of this paper self-identifies as an underrepresented ethnic minority in their field of research or within their geographical location. One or more of the authors of this paper self-identifies as a gender minority in their field of research. One or more of the authors of this paper self-identifies as a member of the LGBTQIA+ community.

Received: May 11, 2022
Revised: March 27, 2023
Accepted: April 14, 2023
Published: April 18, 2023

REFERENCES

1. Charlson, F.J., Ferrari, A.J., Santomauro, D.F., Diminic, S., Stockings, E., Scott, J.G., McGrath, J.J., and Whiteford, H.A. (2018). Global epidemiology and burden of schizophrenia: findings from the global burden of disease study 2016. Schizophr. Bull. *44*, 1195–1203. https://doi.org/10.1093/schbul/sby058.

2. GBD 2017 Disease and Injury Incidence and Prevalence Collaborators (2018). Global, regional, and national incidence, prevalence, and years lived with disability for 354 diseases and injuries for 195 countries and territories, 1990-2017: a systematic analysis for the Global Burden of Disease Study 2017 *392*, 1789–1858. https://doi.org/10.1016/S0140-6736(18)32279-7.

3. Schizophrenia Working Group of the Psychiatric Genomics Consortium (2014). Biological insights from 108 schizophrenia-associated genetic loci. Nature *511*, 421–427. https://doi.org/10.1038/nature13595.

4. Genovese, G., Fromer, M., Stahl, E.A., Ruderfer, D.M., Chambert, K., Landén, M., Moran, J.L., Purcell, S.M., Sklar, P., Sullivan, P.F., et al. (2016). Increased burden of ultra-rare protein-altering variants among 4,877 individuals with schizophrenia. Nat. Neurosci. *19*, 1433–1441. https://doi.org/10.1038/nn.4402.

5. Marshall, C.R., Howrigan, D.P., Merico, D., Thiruvahindrapuram, B., Wu, W., Greer, D.S., Antaki, D., Shetty, A., Holmans, P.A., Pinto, D., et al. (2017). Contribution of copy number variants to schizophrenia from a genome-wide study of 41,321 subjects. Nat. Genet. *49*, 27–35. https://doi.org/10.1038/ng.3725.

6. Singh, T., Walters, J.T.R., Johnstone, M., Curtis, D., Suvisaari, J., Torniainen, M., Rees, E., Iyegbe, C., Blackwood, D., McIntosh, A.M., et al. (2017). The contribution of rare variants to risk of schizophrenia in individuals with and without intellectual disability. Nat. Genet. *49*, 1167–1173. https://doi.org/10.1038/ng.3903.

7. Howrigan, D.P., Rose, S.A., Samocha, K.E., Fromer, M., Cerrato, F., Chen, W.J., Churchhouse, C., Chambert, K., Chandler, S.D., Daly, M.J., et al. (2020). Exome sequencing in schizophrenia-affected parent-offspring trios reveals risk conferred by protein-coding de novo mutations. Nat. Neurosci. *23*, 185–193. https://doi.org/10.1038/s41593-019-0564-3.

8. Lam, M., Chen, C.Y., Li, Z., Martin, A.R., Bryois, J., Ma, X., Gaspar, H., Ikeda, M., Benyamin, B., Brown, B.C., et al. (2019). Comparative genetic architectures of schizophrenia in East Asian and European populations. Nat. Genet. *51*, 1670–1678. https://doi.org/10.1038/s41588-019-0512-x.

9. Singh, T., Poterba, T., Curtis, D., Akil, H., Al Eissa, M., Barchas, J.D., Bass, N., Bigdeli, T.B., Breen, G., Bromet, E.J., et al. (2022). Rare coding variants in ten genes confer substantial risk for schizophrenia. Nature *604*, 509–516. https://doi.org/10.1038/S41586-022-04556-W.

10. Trubetskoy, V., Pardiñas, A.F., Qi, T., Panagiotaropoulou, G., Awasthi, S., Bigdeli, T.B., Bryois, J., Chen, C.Y., Dennison, C.A., Hall, L.S., et al. (2022). Mapping genomic loci implicates genes and synaptic biology in schizophrenia. Nature *604*, 502–508. https://doi.org/10.1038/S41586-022-04434-5.

11. Birnbaum, R., and Weinberger, D.R. (2017). Genetic insights into the neurodevelopmental origins of schizophrenia. Nat. Rev. Neurosci. *18*, 727–740. https://doi.org/10.1038/nrn.2017.125.

12. Hyman, S.E. (2012). Revolution stalled. Sci. Transl. Med. *4*, 155cm11. https://doi.org/10.1126/SCITRANSLMED.3003142.

13. Patel, K.R., Cherian, J., Gohil, K., and Atkinson, D. (2014). Schizophrenia: overview and treatment options. P T *39*, 638–645.

14. Glantz, L.A., and Lewis, D.A. (2000). Decreased dendritic spine density on prefrontal cortical pyramidal neurons in schizophrenia. Arch. Gen. Psychiatr. *57*, 65–73. https://doi.org/10.1001/archpsyc.57.1.65.

15. Finucane, H.K., Reshef, Y.A., Anttila, V., Slowikowski, K., Gusev, A., Byrnes, A., Gazal, S., Loh, P.R., Lareau, C., Shoresh, N., et al. (2018). Heritability enrichment of specifically expressed genes identifies disease-relevant tissues and cell types. Nat. Genet. *50*, 621–629. https://doi.org/10.1038/s41588-018-0081-4.

16. Skene, N.G., Bryois, J., Bakken, T.E., Breen, G., Crowley, J.J., Gaspar, H.A., Giusti-Rodriguez, P., Hodge, R.D., Miller, J.A., Muñoz-Manchado, A.B., et al. (2018). Genetic identification of brain cell types underlying schizophrenia. Nat. Genet. *50*, 825–833. https://doi.org/10.1038/s41588-018-0129-5.

17. Ruzicka, W.B., Mohammadi, S., Davila-Velderrain, J., Subburaju, S., Tso, D.R., Hourihan, M., and Kellis, M. (2020). Single-cell dissection of schizophrenia reveals neurodevelopmental-synaptic axis and transcriptional resilience. Preprint at medRxiv. https://doi.org/10.1101/2020.11.06.20225342.

18. Safari-Alighiarloo, N., Taghizadeh, M., Rezaei-Tavirani, M., Goliaei, B., and Peyvandi, A.A. (2014). Protein-protein interaction networks (PPI) and complex diseases. Gastroenterol. Hepatol. Bed Bench *7*, 17–31.

19. Lage, K. (2014). Protein-protein interactions and genetic diseases: the interactome. Biochim. Biophys. Acta *1842*, 1971–1980. https://doi.org/10.1016/j.bbadis.2014.05.028.

20. Zhang, Y., Pak, C., Han, Y., Ahlenius, H., Zhang, Z., Chanda, S., Marro, S., Patzke, C., Acuna, C., Covy, J., et al. (2013). Rapid single-step induction of functional neurons from human pluripotent stem cells. Neuron *78*, 785–798. https://doi.org/10.1016/j.neuron.2013.05.029.

21. Nehme, R., Zuccaro, E., Ghosh, S.D., Li, C., Sherwood, J.L., Pietilainen, O., Barrett, L.E., Limone, F., Worringer, K.A., Kommineni, S., et al. (2018). Combining NGN2 programming with developmental patterning generates human excitatory neurons with NMDAR-mediated synaptic transmission. Cell Rep. *23*, 2509–2523. https://doi.org/10.1016/j.celrep.2018.04.066.

22. Karczewski, K.J., Francioli, L.C., Tiao, G., Cummings, B.B., Alföldi, J., Wang, Q., Collins, R.L., Laricchia, K.M., Ganna, A., Birnbaum, D.P., et al. (2020). The mutational constraint spectrum quantified from variation in 141,456 humans. Nature *581*, 434–443. https://doi.org/10.1038/s41586-020-2308-7.

23. Kang, H.J., Kawasawa, Y.I., Cheng, F., Zhu, Y., Xu, X., Li, M., Sousa, A.M.M., Pletikos, M., Meyer, K.A., Sedmak, G., et al. (2011). Spatio-temporal transcriptome of the human brain. Nature *478*, 483–489. https://doi.org/10.1038/nature10523.

24. Pintacuda, G., Lassen, F.H., Hsu, Y.-H.H., Kim, A., Martín, J.M., Malolepsza, E., Lim, J.K., Fornelos, N., Eggan, K.C., and Lage, K. (2021). Genoppi is an open-source software for robust and standardized integration of proteomic and genetic data. Nat. Commun. *12*, 2580. https://doi.org/10.1038/s41467-021-22648-5.

25. Li, T., Wernersson, R., Hansen, R.B., Horn, H., Mercer, J., Slodkowicz, G., Workman, C.T., Rigina, O., Rapacki, K., Stærfeldt, H.H., et al. (2017). A scored human protein-protein interaction network to catalyze genomic interpretation. Nat. Methods *14*, 61–64. https://doi.org/10.1038/nmeth.4083.

26. Striessnig, J., Pinggera, A., Kaur, G., Bock, G., and Tuluc, P. (2014). L-type Ca2+ channels in heart and brain. Wiley Interdiscip. Rev. Membr. Transp. Signal. *3*, 15–38. https://doi.org/10.1002/wmts.102.

27. Lundby, A., Rossin, E.J., Steffensen, A.B., Acha, M.R., Newton-Cheh, C., Pfeufer, A., Lynch, S.N., QT Interval International GWAS Consortium QT-IGC, Olesen, S.-P., Brunak, S., et al. (2014). Annotation of loci from genome-wide association studies using tissue-specific quantitative interaction proteomics. Nat. Methods *11*, 868–874. https://doi.org/10.1038/nmeth.2997.

28. Maynard, K.R., Collado-Torres, L., Weber, L.M., Uytingco, C., Barry, B.K., Williams, S.R., Catallini, J.L., Tran, M.N., Besich, Z., Tippani, M., et al. (2021). Transcriptome-scale spatial gene expression in the human dorsolateral prefrontal cortex. Nat. Neurosci. *24*, 425–436. https://doi.org/10.1038/s41593-020-00787-0.

29. Stickels, R.R., Murray, E., Kumar, P., Li, J., Marshall, J.L., Di Bella, D.J., Arlotta, P., Macosko, E.Z., and Chen, F. (2021). Highly sensitive spatial transcriptomics at near-cellular resolution with Slide-seqV2. Nat. Biotechnol. *39*, 313–319. https://doi.org/10.1038/s41587-020-0739-1.

30. Velmeshev, D., Schirmer, L., Jung, D., Haeussler, M., Perez, Y., Mayer, S., Bhaduri, A., Goyal, N., Rowitch, D.H., and Kriegstein, A.R. (2019). Single-cell genomics identifies cell type–specific molecular changes in autism. Science *364*, 685–689. https://doi.org/10.1126/science.aav8130.

31. Koopmans, F., van Nierop, P., Andres-Alonso, M., Byrnes, A., Cijsouw, T., Coba, M.P., Cornelisse, L.N., Farrell, R.J., Goldschmidt, H.L., Howrigan, D.P., et al. (2019). SynGO: an evidence-based, expert-curated knowledge base for the synapse. Neuron *103*, 217–234.e4. https://doi.org/10.1016/j.neuron.2019.05.002.

32. de Leeuw, C.A., Mooij, J.M., Heskes, T., and Posthuma, D. (2015). MAGMA: generalized gene-set analysis of GWAS data. PLoS Comput. Biol. *11*, e1004219. https://doi.org/10.1371/journal.pcbi.1004219.

33. Demontis, D., Walters, R.K., Martin, J., Mattheisen, M., Als, T.D., Agerbo, E., Baldursson, G., Belliveau, R., Bybjerg-Grauholm, J., Bækvad-Hansen, M., et al. (2019). Discovery of the first genome-wide significant risk loci for attention deficit/hyperactivity disorder. Nat. Genet. *51*, 63–75. https://doi.org/10.1038/s41588-018-0269-7.

34. Grove, J., Ripke, S., Als, T.D., Mattheisen, M., Walters, R.K., Won, H., Pallesen, J., Agerbo, E., Andreassen, O.A., Anney, R., et al. (2019). Identification of common genetic risk variants for autism spectrum disorder. Nat. Genet. *51*, 431–444. https://doi.org/10.1038/s41588-019-0344-8.

35. Mullins, N., Forstner, A.J., O'Connell, K.S., Coombes, B., Coleman, J.R.I., Qiao, Z., Als, T.D., Bigdeli, T.B., Børte, S., Bryois, J., et al. (2021). Genome-wide association study of more than 40,000 bipolar disorder cases provides new insights into the underlying biology. Nat. Genet. *53*, 817–829. https://doi.org/10.1038/s41588-021-00857-4.

36. Howard, D.M., Adams, M.J., Clarke, T.-K., Hafferty, J.D., Gibson, J., Shirali, M., Coleman, J.R.I., Hagenaars, S.P., Ward, J., Wigmore, E.M., et al. (2019). Genome-wide meta-analysis of depression identifies 102 independent variants and highlights the importance of the prefrontal brain regions. Nat. Neurosci. *22*, 343–352. https://doi.org/10.1038/s41593-018-0326-7.

37. Lab, N. (2018). UK Biobank GWAS Round 2 Results.

38. Akiyama, M., Ishigaki, K., Sakaue, S., Momozawa, Y., Horikoshi, M., Hirata, M., Matsuda, K., Ikegawa, S., Takahashi, A., Kanai, M., et al. (2019). Characterizing rare and low-frequency height-associated variants in the Japanese population. Nat. Commun. *10*, 4393. https://doi.org/10.1038/s41467-019-12276-5.

39. Sanders, S.J., He, X., Willsey, A.J., Ercan-Sencicek, A.G., Samocha, K.E., Cicek, A.E., Murtha, M.T., Bal, V.H., Bishop, S.L., Dong, S., et al. (2015). Insights into autism spectrum disorder genomic architecture and biology from 71 risk loci. Neuron *87*, 1215–1233. https://doi.org/10.1016/j.neuron.2015.09.016.

40. Satterstrom, F.K., Kosmicki, J.A., Wang, J., Breen, M.S., De Rubeis, S., An, J.Y., Peng, M., Collins, R., Grove, J., Klei, L., et al. (2020). Large-scale exome sequencing study implicates both developmental and functional changes in the neurobiology of autism. Cell *180*, 568–584.e23. https://doi.org/10.1016/j.cell.2019.12.036.

41. Kaplanis, J., Samocha, K.E., Wiel, L., Zhang, Z., Arvai, K.J., Eberhardt, R.Y., Gallone, G., Lelieveld, S.H., Martin, H.C., McRae, J.F., et al. (2020). Evidence for 28 genetic disorders discovered by combining healthcare and

research data. Nature *586*, 757–762. https://doi.org/10.1038/s41586-020-2832-5.

42. Stessman, H.A.F., Xiong, B., Coe, B.P., Wang, T., Hoekzema, K., Fenckova, M., Kvarnung, M., Gerdts, J., Trinh, S., Cosemans, N., et al. (2017). Targeted sequencing identifies 91 neurodevelopmental-disorder risk genes with autism and developmental-disability biases. Nat. Genet. *49*, 515–526. https://doi.org/10.1038/ng.3792.

43. Gallagher, M.D., and Chen-Plotkin, A.S. (2018). The post-GWAS era: from association to function. Am. J. Hum. Genet. *102*, 717–730. https://doi.org/10.1016/j.ajhg.2018.04.002.

44. Schaid, D.J., Chen, W., and Larson, N.B. (2018). From genome-wide associations to candidate causal variants by statistical fine-mapping. Nat. Rev. Genet. *19*, 491–504. https://doi.org/10.1038/s41576-018-0016-z.

45. Broekema, R.V., Bakker, O.B., and Jonkers, I.H. (2020). A practical view of fine-mapping and gene prioritization in the post-genome-wide association era. Open Biol. *10*, 190221. https://doi.org/10.1098/rsob.190221.

46. Mostafavi, H., Spence, J.P., Naqvi, S., and Pritchard, J.K. (2022). Limited overlap of eQTLs and GWAS hits due to systematic differences in discovery. Preprint at bioRxiv. https://doi.org/10.1101/2022.05.07.491045.

47. Benarroch, E.E. (2013). HCN channels: function and clinical implications. Neurology *80*, 304–310. https://doi.org/10.1212/WNL.0b013e31827dec42.

48. Palmer, D.S., Howrigan, D.P., Chapman, S.B., Adolfsson, R., Bass, N., Blackwood, D., Boks, M.P.M., Chen, C.-Y., Churchhouse, C., Corvin, A.P., et al. (2022). Exome sequencing in bipolar disorder identifies AKAP11 as a risk gene shared with schizophrenia. Nat. Genet. *54*, 541–547. https://doi.org/10.1038/s41588-022-01034-x.

49. Sekar, A., Bialas, A.R., de Rivera, H., Davis, A., Hammond, T.R., Kamitaki, N., Tooley, K., Presumey, J., Baum, M., Van Doren, V., et al. (2016). Schizophrenia risk from complex variation of complement component 4. Nature *530*, 177–183. https://doi.org/10.1038/nature16549.

50. Yilmaz, M., Yalcin, E., Presumey, J., Aw, E., Ma, M., Whelan, C.W., Stevens, B., McCarroll, S.A., and Carroll, M.C. (2021). Overexpression of schizophrenia susceptibility factor human complement C4A promotes excessive synaptic loss and behavioral changes in mice. Nat. Neurosci. *24*, 214–224. https://doi.org/10.1038/s41593-020-00763-8.

51. Bantscheff, M., Schirle, M., Sweetman, G., Rick, J., and Kuster, B. (2007). Quantitative mass spectrometry in proteomics: a critical review. Anal. Bioanal. Chem. *389*, 1017–1031. https://doi.org/10.1007/s00216-007-1486-6.

52. Freeman, W.M., and Hemby, S.E. (2004). Proteomics for protein expression profiling in neuroscience. Neurochem. Res. *29*, 1065–1081. https://doi.org/10.1023/b:nere.0000023594.21352.17.

53. Kenworthy, A.K. (2001). Imaging protein-protein interactions using fluorescence resonance energy transfer microscopy. Methods *24*, 289–296. https://doi.org/10.1006/meth.2001.1189.

54. Clowsley, A.H., Kaufhold, W.T., Lutz, T., Meletiou, A., Di Michele, L., and Soeller, C. (2020). Detecting nanoscale distribution of protein pairs by proximity-dependent super-resolution microscopy. J. Am. Chem. Soc. *142*, 12069–12078. https://doi.org/10.1021/jacs.9b03418.

55. Gilmore, B.L., Winton, C.E., Demmert, A.C., Tanner, J.R., Bowman, S., Karageorge, V., Patel, K., Sheng, Z., and Kelly, D.F. (2015). A molecular toolkit to visualize native protein assemblies in the context of human disease. Sci. Rep. *5*, 14440. https://doi.org/10.1038/srep14440.

56. Pintacuda, G., Hsu, Y.-H.H., Tsafou, K., Li, K.W., Martín, J.M., Riseman, J., Biagini, J.C., Ching, J.K.T., Mena, D., Gonzalez-Lozano, M.A., et al. (2023). Protein interaction studies in human induced neurons indicate convergent biology underlying autism spectrum disorders. Cell Genom. *3*, 100250. https://doi.org/10.1016/j.xgen.2022.100250.

57. Lam, M., Awasthi, S., Watson, H.J., Goldstein, J., Panagiotaropoulou, G., Trubetskoy, V., Karlsson, R., Frei, O., Fan, C.-C., De Witte, W., et al. (2020). RICOPILI: rapid imputation for COnsortias PIpeLIne. Bioinformatics *36*, 930–933. https://doi.org/10.1093/bioinformatics/btz633.

58. Quinn, T.P., Richardson, M.F., Lovell, D., and Crowley, T.M. (2017). Propr: an R-package for identifying proportionally abundant features using compositional data analysis. Sci. Rep. *7*, 16252. https://doi.org/10.1038/s41598-017-16520-0.

59. Chang, C.C., Chow, C.C., Tellier, L.C., Vattikuti, S., Purcell, S.M., and Lee, J.J. (2015). Second-generation PLINK: rising to the challenge of larger and richer datasets. GigaScience *4*, 7. https://doi.org/10.1186/s13742-015-0047-8.

60. Williams, H.J., Norton, N., Dwyer, S., Moskvina, V., Nikolov, I., Carroll, L., Georgieva, L., Williams, N.M., Morris, D.W., Quinn, E.M., et al. (2011). Fine mapping of ZNF804A and genome-wide significant evidence for its involvement in schizophrenia and bipolar disorder. Mol. Psychiatr. *16*, 429–441. https://doi.org/10.1038/mp.2010.36.

61. Gillis, J., Burashnikov, E., Antzelevitch, C., Blaser, S., Gross, G., Turner, L., Babul-Hirji, R., and Chitayat, D. (2012). Long QT, syndactyly, joint contractures, stroke and novel CACNA1C mutation: expanding the spectrum of Timothy syndrome. Am. J. Med. Genet. *158A*, 182–187. https://doi.org/10.1002/ajmg.a.34355.

62. Lesca, G., Rudolf, G., Bruneau, N., Lozovaya, N., Labalme, A., Boutry-Kryza, N., Salmi, M., Tsintsadze, T., Addis, L., Motte, J., et al. (2013). GRIN2A mutations in acquired epileptic aphasia and related childhood focal epilepsies and encephalopathies with speech and language dysfunction. Nat. Genet. *45*, 1061–1066. https://doi.org/10.1038/ng.2726.

63. Hamdan, F.F., Gauthier, J., Spiegelman, D., Noreau, A., Yang, Y., Pellerin, S., Dobrzeniecka, S., Côté, M., Perreau-Linck, E., Carmant, L., et al. (2009). Mutations in SYNGAP1 in autosomal nonsyndromic mental retardation. N. Engl. J. Med. *360*, 599–605. https://doi.org/10.1056/NEJMoa0805392.

64. Deciphering Developmental Disorders Study (2017). Prevalence and architecture of de novo mutations in developmental disorders. Nature *542*, 433–438. https://doi.org/10.1038/nature21062.

65. Zweier, C., Peippo, M.M., Hoyer, J., Sousa, S., Bottani, A., Clayton-Smith, J., Reardon, W., Saraiva, J., Cabral, A., Gohring, I., et al. (2007). Haploinsufficiency of TCF4 causes syndromal mental retardation with intermittent hyperventilation (Pitt-Hopkins syndrome). Am. J. Hum. Genet. *80*, 994–1001. https://doi.org/10.1086/515583.

66. Cukier, H.N., Dueker, N.D., Slifer, S.H., Lee, J.M., Whitehead, P.L., Lalanne, E., Leyva, N., Konidari, I., Gentry, R.C., Hulme, W.F., et al. (2014). Exome sequencing of extended families with autism reveals genes shared across neurodevelopmental and neuropsychiatric disorders. Mol. Autism. *5*, 1. https://doi.org/10.1186/2040-2392-5-1.

67. Döcker, D., Schubach, M., Menzel, M., Munz, M., Spaich, C., Biskup, S., and Bartholdi, D. (2014). Further delineation of the SATB2 phenotype. Eur. J. Hum. Genet. *22*, 1034–1039. https://doi.org/10.1038/ejhg.2013.280.

68. Zarate, Y.A., Perry, H., Ben-Omran, T., Sellars, E.A., Stein, Q., Almureikhi, M., Simmons, K., Klein, O., Fish, J., Feingold, M., et al. (2015). Further supporting evidence for the SATB2-associated syndrome found through whole exome sequencing. Am. J. Med. Genet. *167A*, 1026–1032. https://doi.org/10.1002/ajmg.a.36849.

69. Yi, F., Danko, T., Botelho, S.C., Patzke, C., Pak, C., Wernig, M., and Südhof, T.C. (2016). Autism-associated SHANK3 haploinsufficiency causes Ih channelopathy in human neurons. Science *352*, aaf2669. https://doi.org/10.1126/science.aaf2669.

70. Cross-Disorder Group of the Psychiatric Genomics Consortium (2013). Identification of risk loci with shared effects on five major psychiatric disorders: a genome-wide analysis. Lancet *381*, 1371–1379. https://doi.org/10.1016/S0140-6736(12)62129-1.

71. Ferreira, M.A.R., O'Donovan, M.C., Meng, Y.A., Jones, I.R., Ruderfer, D.M., Jones, L., Fan, J., Kirov, G., Perlis, R.H., Green, E.K., et al. (2008). Collaborative genome-wide association analysis supports a role for ANK3 and CACNA1C in bipolar disorder. Nat. Genet. *40*, 1056–1058. https://doi.org/10.1038/ng.209.

72. Won, H., De La Torre-Ubieta, L., Stein, J.L., Parikshak, N.N., Huang, J., Opland, C.K., Gandal, M.J., Sutton, G.J., Hormozdiari, F., Lu, D., et al. (2016). Chromosome conformation elucidates regulatory

relationships in developing human brain. Nature *538*, 523–527. https://doi.org/10.1038/nature19847.

73. Mellacheruvu, D., Wright, Z., Couzens, A.L., Lambert, J.-P., St-Denis, N.A., Li, T., Miteva, Y.V., Hauri, S., Sardiu, M.E., Low, T.Y., et al. (2013). The CRAPome: a contaminant repository for affinity purification-mass spectrometry data. Nat. Methods *10*, 730–736. https://doi.org/10.1038/nmeth.2557.

74. Ritchie, M.E., Phipson, B., Wu, D., Hu, Y., Law, C.W., Shi, W., and Smyth, G.K. (2015). Limma powers differential expression analyses for RNA-sequencing and microarray studies. Nucleic Acids Res. *43*, e47. https://doi.org/10.1093/nar/gkv007.

75. Skinnider, M.A., Squair, J.W., and Foster, L.J. (2019). Evaluating measures of association for single-cell transcriptomics. Nat. Methods *16*, 381–386. https://doi.org/10.1038/s41592-019-0372-4.

76. Yates, A.D., Achuthan, P., Akanni, W., Allen, J., Allen, J., Alvarez-Jarreta, J., Amode, M.R., Armean, I.M., Azov, A.G., Bennett, R., et al. (2020). Ensembl 2020. Nucleic Acids Res. *48*, D682–D688. https://doi.org/10.1093/nar/gkz966.

77. 1000 Genomes Project Consortium, Auton, A., Brooks, L.D., Durbin, R.M., Garrison, E.P., Kang, H.M., Korbel, J.O., Marchini, J.L., McCarthy, S., McVean, G.A., and Abecasis, G.R. (2015). A global reference for human genetic variation. Nature *526*, 68–74. https://doi.org/10.1038/nature15393.

78. Viechtbauer, W. (2010). Conducting meta-analyses in R with the metafor package. J. Stat. Software *36*. https://doi.org/10.18637/jss.v036.i03.

79. Carvalho-Silva, D., Pierleoni, A., Pignatelli, M., Ong, C., Fumis, L., Karamanis, N., Carmona, M., Faulconbridge, A., Hercules, A., McAuley, E., et al. (2019). Open Targets Platform: new developments and updates two years on. Nucleic Acids Res. *47*, D1056–D1065. https://doi.org/10.1093/nar/gky1133.

80. Mendez, D., Gaulton, A., Bento, A.P., Chambers, J., De Veij, M., Félix, E., Magariños, M.P., Mosquera, J.F., Mutowo, P., Nowotka, M., et al. (2019). ChEMBL: towards direct deposition of bioassay data. Nucleic Acids Res. *47*, D930–D940. https://doi.org/10.1093/nar/gky1075.

STAR★METHODS

KEY RESOURCES TABLE

REAGENT or RESOURCE	SOURCE	IDENTIFIER
Antibodies		
ACTB	Abcam	Cat# ab8227; RRID: AB_2305186
AKAP11	Invitrogen	Cat# PA5-103369; RRID: AB_2852713
APLP2	Proteintech Group	Cat# 15041-1-AP; RRID: AB_2289597
ARID3B	Fortis Life Sciences	Cat# A302-565A; RRID: AB_2034823
C3	Abcam	Cat# ab97462; RRID: AB_10679468
CACNA1C	Alomone Labs	Cat# ACC-003; RRID: AB_2039771
CACNB2	Abnova	Cat# H00000783-A01; RRID: AB_463642
CACNB3	Alomone Labs	Cat# ACC-008: RRID: AB_2039787
CAMK2D	Abcam	Cat# ab181052; RRID: AB_2891241
CHD4	Abcam	Cat# ab70469; RRID: AB_2229454
CKB	Santa Cruz Biotechnology	Cat# sc-374072; RRID: AB_10947239
CNTNAP1	Abcam	Cat# ab34151; RRID: AB_869934
COPS2	Proteintech Group	Cat# 10969-2-AP; RRID: AB_2276346
COPS5	Cell Signaling Technology	Cat# 6895; RRID: AB_10839271
CSMD1	Abcam	Cat# ab166908
CTNND1	Santa Cruz Biotechnology	Cat# sc-23873; RRID: AB_2086394
CUL3	Fortis Life Sciences	Cat# A301-109A; RRID: AB_873023
ELAVL2	Proteintech Group	Cat# 14008-1-AP; RRID: AB_2096356
ELAVL3	ABclonal	Cat# A6091; RRID: AB_2766743
EPN2	Fortis Life Sciences	Cat# A305-510A; RRID: AB_2891436
FMR1 (FMRP)	Abcam	Cat# ab17722; RRID: AB_2278530
FXR1	Proteintech Group	Cat# 13194-1-AP; RRID: AB_2110702
GABBR2 (GABAB2)	Abcam	Cat# ab75838; RRID: AB_1310245

(*Continued on next page*)

Continued

REAGENT or RESOURCE	SOURCE	IDENTIFIER
GNAO1	Abcam	Cat# ab154001
GRIN2A	Abcam	Cat# ab133265; RRID: AB_11158532
HCN1	Proteintech Group	Cat# 55222-1-AP; RRID: AB_11182929
HCN4	Abcam	Cat# ab32675; RRID: AB_732770
HNRNPA2B1	Abcam	Cat# ab6102; RRID: AB_305293
IGF2BP1	Proteintech Group	Cat# 22803-1-AP; RRID: AB_2879173
IGF2BP2	Abcam	Cat# ab124930; RRID: AB_11131218
IGF2BP3	Fortis Life Sciences	Cat# A303-426A; RRID: AB_10951696
INA	Fortis Life Sciences	Cat# A305-441A; RRID: AB_2631832
ISL1	Abcam	Cat# ab109517; RRID: AB_10866454
KIAA1549	Fortis Life Sciences	Cat# A305-877A; RRID: AB_2891771
LDB1	Novus Biologicals	Cat# NBP1-77832; RRID: AB_11038158
MARK3	LSBio	Cat# LS-B5226; RRID: AB_10851098
MEF2C	Atlas Antibodies	Cat# AMAb90727; RRID: AB_2665645
MSI2	Abcam	Cat# ab76148; RRID: AB_1523981
NEGR1	Proteintech Group	Cat# 13674-1-AP; RRID: AB_2877969
NSG1	Millipore Sigma	Cat# SAB4501190; RRID: AB_10745270
PARP1	Proteintech Group	Cat# 13371-1-AP; RRID: AB_2160459
PCDHA2	Proteintech Group	Cat# 10127-2-AP; RRID: AB_2158964
PCDHB5	Proteintech Group	Cat# 19609-1-AP; RRID: AB_10792248
PCM1	Fortis Life Sciences	Cat# A301-150A; RRID: AB_873100
PDE4B	Cell Signaling Technology	Cat# 72096S; RRID: AB_2799812
PYGB	Proteintech Group	Cat# 12075-1-AP; RRID: AB_2174885
RALY	Abcam	Cat# ab170105
RIMS1	Proteintech Group	Cat# 24576-1-AP; RRID: AB_2879618

(*Continued on next page*)

Continued

REAGENT or RESOURCE	SOURCE	IDENTIFIER
RIMS1	Santa Cruz Biotechnology	Cat# sc-368540
RUNX1T1	Abcam	Cat# ab124269; RRID: AB_10976059
SEMA4C	Santa Cruz Biotechnology	Cat# sc-136445; RRID: AB_10837020
SF3B1	Cell Signaling Technology	Cat# 14434S; RRID: AB_2798479
SRPK2	Fortis Life Sciences	Cat# A302-467A; RRID: AB_1944286
SYNGAP1	Cell Signaling Technology	Cat# 5539; RRID: AB_10694401
TCF4	GeneTex	Cat# GTX17912; RRID: AB_2887569
XRCC5	Abcam	Cat# ab80592; RRID: AB_1603758
XRCC6	Abcam	Cat# ab92450; RRID: AB_10562280
V5 tag	MBL	Cat# M167-11
Mouse IgG1 monoclonal isotype control	Cell Signaling Technology	Cat# 5415; RRID: AB_10829607
Mouse IgG2a monoclonal isotype control	Cell Signaling Technology	Cat# 61656; RRID: AB_2799613
Rabbit IgG monoclonal isotype control	Cell Signaling Technology	Cat# 3900; RRID: AB_1550038
Rabbit IgG polyclonal isotype control	Sigma-Aldrich	Cat# I5006; RRID: AB_1163659
Chemicals, peptides, and recombinant proteins		
Accutase	Gibco	Cat# A11105
Agilent RNA 6000 Pico kit	Agilent Technologies	Cat# 5067-1513
Ambion DNA-free DNase Treatment kit	Life Technologies	Cat# AM1906
B-27 supplement	Thermo Scientific	Cat# 17504044
BDNF	R&D Systems	Cat# 248-BD/CF
2100 Bioanalyzer Instrument	Agilent Technologies	Cat# G2939BA
Blotting-Grade Blocker	Bio-Rad Laboratories	Cat# 1706404
CNTF	R&D Systems	Cat# 257-NT
CryoStor CS10	Stem Cell Technologies	Cat# 07930
DMEM/F - 12	Life Technologies	Cat# 11320033
Doxycycline hyclate	Sigma-Aldrich	Cat# 24390-14-5
Fetal Bovine Serum	R&D Systems	Cat# S11195
GDNF	R&D Systems	Cat# 212-GD
Geltrex	Life Technologies	Cat# A1413301
Geneticin	Gibco	Cat# 10131027
D-(+)-Glucose	Sigma-Aldrich	Cat# 50-99-7
Glutamax	Life Technologies	Cat# 35050079
Gridded Plate 150 x 25 mm	VWR International	Cat# 25383-103

(*Continued on next page*)

Continued

REAGENT or RESOURCE	SOURCE	IDENTIFIER
Halt™ Protease and Phosphatase Inhibitor	Thermo Scientific	Cat# 78442
Laminin, Mouse	VWR International	Cat# 47743-734
LDN-193189	Stem Cell Technologies	Cat# 1435934-00-1
MEM NEAA	Life Technologies	Cat# 11140076
Methanol ≥99.8%	Fisher Scientific	Cat# 67-56-1
N-2 Supplement	Life Technologies	Cat# 17502048
Neurobasal	Life Technologies	Cat# 21103049
Normocin	Invitrogen	Cat# ant-nr-2
NuPAGE™ 12%, Bis-Tris Gel	Invitrogen	Cat# NP0341PK2
NuPAGE Transfer Buffer (20X)	Life Technologies	Cat# NP00061
PBS	Life Technologies	Cat# 10010049
PVDF/Filter Paper Sandwich	Life Technologies	Cat# LC2002
ROCK Inhibitor (Y-27632)	Stemgent	Cat# 04-0012
SB 431542	Tocris	Cat# 1614
StemFlex™ Medium	Life Technologies	Cat# A3349401
Microcentrifuge Tubes	VWR International	Cat# 0011-702
Sterile Sleeves	VWR International	Cat# 414004-510
Trizol	Life Technologies	Cat# 15596026
TruSeq Stranded Total RNA Library Prep Kit	Illumina	Cat# 20020596
TrypLE	Life Technologies	Cat# 12604039
Trypsin	Promega	Cat# V5111
XAV939	Stemgent	Cat# 04-00046
Critical commercial assays		
Pierce™ Protein A/G Magnetic Beads	Thermo Scientific	Cat# 88803
SuperSignal™ West Femto Maximum Sensitivity Substrate	Thermo Scientific	Cat# 34094
Pierce™ IP Lysis Buffer	Thermo Scientific	Cat# 87788
EnGen Spy Cas9 NLS	New England Biolabs	Cat# M0646T
Deposited data		
IP-MS data	This study	MassIVE: MSV000087514
Experimental Models: Cell lines		
iPS line from human fibroblasts with integrated *NGN2*	Novartis Institutes for BioMedical Research	iPS hDFn 83/22 iNgn2#9; iPS3 in Nehme et al.[21]
Human embryonic stem cells WA01	WiCell	WA01 H1; NIH registration no. 0043
Software and algorithms		
Ricopili	Lam et al.[57]	https://data.broadinstitute.org/mpg/ricopili/
Spectrum Mill (v7.0)	Broad Proteomics Platform	https://proteomics.broadinstitute.org
Genoppi (v1.0)	Pintacuda et al.[24]	https://github.com/lagelab/Genoppi
propr (v4.2.6)	Quinn et al.[58]	https://github.com/tpq/propr
MAGMA (v1.09b)	deLeeuw et al.[32]	https://ctg.cncr.nl/software/magma
PLINK (v1.9)	Chang et al.[59]	https://www.cog-genomics.org/plink/
Custom code	This study	https://github.com/lagelab/SCZ_PPI; https://doi.org/10.5281/zenodo.7814403

RESOURCE AVAILABILITY

Lead contact

Further information and requests for resources and reagents should be directed to and will be fulfilled by the lead contact, Kasper Lage (lage.kasper@mgh.harvard.edu).

Materials availability

This study did not generate new unique reagents.

Data and code availability

- The original mass spectra and sequence database used for searches have been deposited at MassIVE (MSV000087514) and are publicly available as of the date of publication.
- All original code has been deposited at GitHub (https://github.com/lagelab/SCZ_PPI) and Zenodo (https://doi.org/10.5281/zenodo.7814403) and is publicly available as of the date of publication.
- Any additional information required to reanalyze the data reported in this paper is available from the lead contact upon request.

EXPERIMENTAL MODEL AND SUBJECT DETAILS

Cell lines

iNs

iNs collected at time points under one week of differentiation were dissociated from plates with Accutase (Innovative Cell Technologies AT104-500) at 37°C for 5-10 min. iNs collected at time points beyond two weeks of differentiation were collected by removing media, adding 1x PBS, and swirling the plates until the neurons detached. Dissociated or detached cells were collected in 15 mL or 50 mL Falcon tubes depending on the number of cells and washed 3 times. Each wash consisted of centrifugation at 300 RCF for 3-5 min, discarding of the supernatant, and resuspension of the cell pellet in 1x PBS. After the final wash, the sample was centrifuged at 300 RCF for 3-5 min, supernatant was discarded, and cells were either lysed or flash frozen in liquid nitrogen and stored at -80°C. Lysis was performed according to manufacturer's protocol using Pierce IP lysis buffer (Thermo Scientific #87788) with 1x Halt Protease and Phosphatase cocktail inhibitor (Thermo Scientific #7844). Protein concentration of the lysate was quantified using BCA Protein assay (Thermo Scientific #23227). When not used for IP-MS experiments, the lysate was aliquoted in low-bind microfuge tubes (Axygen Scientific #MCT-175-L-C), flash frozen and stored at -80°C.

Cancer and HEK cells

We used the following cell lines as controls in western blots: HEK-293 (ATCC CRL-1573), a human embryonic kidney cell line; TF-1 (ATCC CRL-2003), a human erythroleukemia cell line; K-562 (ATCC CCL-243), a human myelogenous leukemia cell line; and U-937 (ATCC CRL-1593.2), a histiocytic lymphoma cell line. All cell lines were grown on uncoated plates (Corning) according to vendor recommendations. Media was changed every 3 days and cells were passaged when reaching 70% confluency. All cell lines were incubated at 37 °C, 5% CO_2. TrypLE (Thermo Scientific) was used to detach cells from plates.

Mouse cortex sample

Mouse cortices were isolated from p0 pups of C57BL/6 background, cut into small pieces, and flash frozen. Lysis was performed by adding Pierce IP lysis buffer to frozen pieces and immediately applying a handheld homogenizer (VWR pellet mixer #47747-370). All subsequent steps were the same as those for iNs.

METHOD DETAILS

iN differentiation

Glutamatergic patterned induced neurons (iNs) were differentiated from male stem cells by conditional expression of the neuralizing transcription factor NGN2 as previously described,[21] with the exception that N2 media was used instead of KSR media during days 0 to 3. iNs were re-passaged at day 3 of differentiation (i.e., 40,000 cells/cm2) on Geltrex (Thermo Scientific #A1413202) coated plates. To remove remaining proliferating cells, fluoro-deoxyuridine (Bioworld 40690016-2) was added to cell cultures at 10 μM on day 6 of differentiation. iNs used in a subset of the CACNA1C, HCN1, and TCF4 IP-MS experiments (Table S5) were differentiated from human embryonic stem cells WA01 (H1, NIH registration no.

0043) transduced with lentiviruses carrying TetO::Ngn2-Puro and reverse tetracycline-controlled transactivator (rtTA), custom-packaged by Alstem. All other IP-MS experiments used iNs generated from a clonally selected induced PSC line (iPS hDFn 83/22 iNgn2#9 [iPS3]) with TetO::Ngn2 and rtTA delivered via PiggyBAC.[21]

Western blotting

For western blots, frozen lysates were thawed on ice, diluted to desired concentration in 1x PBS, and brought to 1x LDS using 4x LDS stock. Samples were denatured at various conditions based on what we identified to work best for each protein of interest. Prepared samples were run on NuPAGE 1.5mm 3-7% Tris-Acetate or 1mm 4-12% Bis-Tris gels (Thermo Scientific). Transfer was onto a nitrocellulose membrane using XCell wet transfer (Invitrogen), iBlot2 (Thermo Scientific), or Trans-Blot Turbo (BioRad). Membranes were blocked with 5% BSA or 5% milk diluted in TBST, incubated with primary antibody diluted in matching blocking buffer for at least 12 hat 4°C, and washed 3 x 10 min in TBST. Membranes were incubated with HRP-conjugated secondary antibody diluted in 5% milk for 1h at RT, washed 3 x 10 min in TBST, developed with enhanced chemiluminescent substrate (Thermo Scientific #34095), and imaged on ChemiDoc MP (BioRad). In 'forward' IP western validation, the immunoprecipitate of the index protein was loaded into the gel and incubated with the primary antibody of an interactor protein to determine if the interactor could be found in the immunoprecipitate; in 'reverse' IP western validation, the immunoprecipitate of an interactor was loaded into the gel and incubated with the primary antibody of the index protein to determine if the index protein could be found in the immunoprecipitate. Western blot antibodies used for each protein of interest are listed in Table S4.

Immunoprecipitations

For immunoprecipitations (IPs) followed by western blots or Coomassie stain analysis, either fresh or previously frozen lysates were used. For IPs followed by mass spectrometry (MS) only fresh lysates were used. On day 1, the needed amounts of lysate and IP antibody were added to a 1.7 mL Axygen MaxyClear tube (MCT-175-L-C), then brought to a final volume of 1.3 mL with Pierce IP lysis buffer. Tubes were then rotated at 4°C overnight for 14-18 h. On day 2, the needed amount of beads per IP were apportioned to separate tubes, washed twice in cold lysis buffer, resuspended in 200 µL lysis buffer per tube, added to corresponding tubes, and rotated at 4°C for 2-4 h. After incubation, tubes were placed on ice, and beads were first washed once in 1mL cold lysis buffer and then twice in 1x cold PBS. To remove supernatants in between the steps, magnetic beads were placed on a magnetic rack on ice and agarose beads were spun at 2,000 x g for 3 min. Supernatants after overnight rotation and each wash step were collected for western blot analysis of IP quality. After the third wash, supernatant was removed, and beads were resuspended in 50 µL of PBS if the IP was to be processed by MS and 40 µL of PBS if the IP was to be processed by western blot or Coomassie stain. Samples were flash frozen in liquid nitrogen and stored at -80°C until further use. All IP experiments sent for MS consisted of 4 IP samples performed on cells from the same differentiation batch: 2 replicate experimental IPs using an antibody against the protein of interest (i.e., an index protein) and 2 replicate control IPs using a control IgG antibody. IP antibodies used for each protein of interest are listed in Table S4.

Immunoprecipitations using V5 epitope tagged TCF4

For immunoprecipitation of TCF4, an ORF of the TCF4 isoform A with a c-terminal V5-tag was acquired from the Broad Institute Genetic Perturbation Platform, and lentiviruses were generated from the construct by ALSTEM Inc. Lentiviruses were delivered to iN cultures at a multiplicity of infection (MOI) of 4 at day 3 of differentiation during re-passaging, and mock-transduced cells were used as controls. Cells were collected at day 6 of differentiation by washing 3 times with PBS, followed by lysis and scraping on the plate. Lysates were then processed and quantified as usual. For IP, the needed amount of lysate was added to a microfuge tube and brought to a final volume of 1.3 mL with Pierce IP lysis buffer, then incubated overnight with anti-v5 antibody directly coupled to magnetic beads (MBL International, M167-11). The remaining protocol is the same as used for the other IPs.

Mass spectrometry

Sample preparation

Proteins were digested on beads using 90 µl of digestion buffer (2 M urea/50 mM Tris buffer with 1 mM DTT and 5 µg/mL Trypsin) for 1 hr, shaking at 1000 rpm. The suspension was then transferred to a new tube, and

the beads were washed twice with 60 μL of wash buffer (2 M urea/50 mM Tris buffer). The wash buffer was added to the suspension with digestion. The digestion and wash process were repeated a second time pooling the suspensions with the suspensions from the first round. The pooled solution was reduced using 4 mM DTT for 30 minat 25°C shaking at 1000 rpm. The proteins were then alkylated using 10 mM iodoacetamide and incubating for 45 minat 25°C shaking at 1000 rpm and protected from light. Proteins were then digested with 0.5 μg of trypsin overnight at 25°C shaking at 700 rpm. The next day proteins were quenched using 40 μL of 10% formic acid and desalted using an Oasis Cartridge. Samples were vacuum dried and labeled with iTRAQ4 (Sciex Inc.) or TMT10 (Thermo Scientific) kits. Each iTRAQ 4-plex consisted of 2 replicate experimental IPs using an antibody against the protein of interest (i.e., an index protein), and 2 replicate control IPs using a control IgG antibody. The specific iTRAQ labels for each replicate pair are indicated in Table S5. For 'RIMS1_wk4_2', a TMT 10-plex experiment was conducted with antibodies from Santa Cruz Biotechnology (SC; 128C, 129N), Proteintech Group (PT; 126, 127N), and Synaptic Systems (SYSY; 129C, 130N). Two sets of replicate control IPs were included for PT (127C, 128N) and SC/SYSY (130C, 131). Only the results from the SC antibody met our quality control metrics and were reported.

Liquid chromatography-tandem mass spectrometry (LC-MS/MS)

Reconstituted peptides were separated on an online nanoflow EASY-nLC 1000 UHPLC system (Thermo Scientific) and analyzed on a benchtop Orbitrap Q Exactive Plus mass spectrometer (Thermo Scientific). The peptide samples were injected onto a capillary column (Picofrit with 10 μm tip opening/75 μm diameter, New Objective, PF360-75-10-N-5) packed in-house with 20 cm C18 silica material (1.9 μm ReproSil-Pur C18-AQ medium, Dr. Maisch GmbH, r119.aq). The UHPLC setup was connected with a custom-fit microadapting tee (360 μm, IDEX Health & Science, UH-753), and capillary columns were heated to 50 °C in column heater sleeves (Phoenix-ST) to reduce backpressure during UHPLC separation. Injected peptides were separated at a flow rate of 200 nL/min with a linear 150 min gradient from 94% solvent A (3% acetonitrile, 0.1% formic acid) to 35% solvent B (90% acetonitrile, 0.1% formic acid), followed by a linear 8 min gradient from 35% solvent B to 60% solvent B and a 3 min ramp to 90% B. The Q Exactive instrument was operated in the data-dependent mode acquiring HCD MS/MS scans (R=17,500 for iTRAQ4, or R=35,000 for TMT10) after each MS1 scan (R=70,000) on the 12 most abundant ions using an MS1 ion target of 3x106 ions and an MS2 target of 5x104 ions. The maximum ion time utilized for the MS/MS scans was 120 ms; the HCD-normalized collision energy was set to 28 for iTRAQ4 or 31 for TMT10; the dynamic exclusion time was set to 20s, and the peptide match and isotope exclusion functions were enabled.

QUANTIFICATION AND STATISTICAL ANALYSIS

Refining geneticdata to identify index genes

Three-step procedure for selecting index genes

Starting with 125 independent autosomal SNPs that reached genome-wide significance in the combined discovery-replication meta-analysis of the PGC schizophrenia GWAS[3] (phase 2), Ricopili[57] (https://data.broadinstitute.org/mpg/ricopili/) was used to map the 124 non-MHC (major histocompatibility complex) region SNPs to 445 genes (Set 1; Table S1) in linkage disequilibrium (LD) loci, whose boundaries were defined by SNPs in LD (r^2> 0.6) with the index SNPs, ±50kb on either end. Next, we excluded SNPs in intergenic regions or in loci with multiple protein-coding genes, resulting in a list of 40 SNPs pointing to 37 unique protein-coding genes (Set 2) in single-gene loci. We further refined the 37 genes into a set of 10 genes (Set 3) based on strong orthogonal evidence supporting their involvement in psychiatric diseases (see below). We also included *SYNGAP1* in the MHC region (which was excluded from the SNP-to-gene mapping process due to its LD complexity) in all 3 sets based on strong orthogonal evidence. In total, we identified 11 high-confidence schizophrenia risk genes and considered their encoded proteins as index proteins in the proteomic experiments.

Orthogonal evidence for the index genes

The index genes were selected based on several types of orthogonal genetic or functional evidence, including: i] high-density genotyping experiments of individual genes (*ZNF804A*),[60] ii] sequencing or copy number variant studies linking genes to autism spectrum disorders or neurodevelopmental delay (*CACNA1C*, *CUL3*, *CSMD1*, *GRIN2A*, *SATB2 SYNGAP1*, *TCF4*),[39,61–68] iii] strong functional evidence supporting that the gene in question is causal (*HCN1*),[69] and iv] multiple subunits from the same protein complex are encoded by genes in different single-gene loci linked to psychiatric diseases (*CACNA1C*, *CACNB2*, *RIMS1*).[3,70,71] In addition, we annotated the 10 genes prioritized from single-gene GWAS loci

using Hi-C chromatin interaction data from the developing human brain,[72] which may point to long-range regulation of genes outside of the loci in the context of schizophrenia; only three of these genes (*CUL3*, *RIMS1*, *SATB2*) lie in loci that exclusively interacted with long-range genes outside of the loci (Table S1).

pLI score enrichment analysis

We extracted pLI scores from the gnomAD[22] (v2.1.1) 'pLoF Metrics by Gene TSV' dataset. We performed one-tailed Kolmogorov-Smirnov (KS) tests to assess whether various gene sets are enriched for high pLI scores compared to other genes in the genome. The tested gene sets include: i] SCHEMA[9] genes with FDR <3.7e-3 (exome-wide significance) and 0.5, ii] Sets 1-3 defined by our index gene selection steps, and iii] genes in PGC schizophrenia GWAS (phase 3) loci[10] and subsets of these genes prioritized by FINEMAP/SMR analysis and/or our interaction data (see social manhattan plot). In addition, we performed one-tailed KS tests to compare the pLI scores of several gene sets that are subsets and supersets of each other, and two-tailed KS tests to compare a few disjoint sets. Table S2 summarizes all the comparisons performed. Finally, we also performed one-tailed KS tests to assess whether the stringent interactors in our interaction networks (Table S9) have enriched pLI scores compared to the non-interactors linked to each network.

BrainSpan expression profiles

We obtained gene expression data in four distinct parts of the frontal cortex (dorsolateral prefrontal cortex [DFC], medial prefrontal cortex [MFC], ventrolateral prefrontal cortex [VFC], orbital frontal cortex [OFC]) across 10 developmental stages from the BrainSpan (https://www.brainspan.org) exon microarray dataset.[23] At each developmental stage, we calculated the median and standard error of the expression values for various genes or gene sets including: i] SCHEMA genes with FDR <3.7e-3, 0.05, 0.25, and 0.5, ii] Sets 1-3 defined by our index gene selection steps, iii] index and interactor genes in our combined network of all IPs (Table S9), iv] genes in PGC schizophrenia GWAS (phase 3) loci and subsets of these genes prioritized by FINEMAP/SMR analysis and/or our interaction data (see social manhattan plot), and v] random genes sampled from the BrainSpan dataset for comparison against the other gene sets. Table S3 provides more detailed summary statistics for all gene sets.

IP-MS data analysis

Spectrum Mill analysis

All mass spectra were processed using Spectrum Mill (v7.0; https://proteomics.broadinstitute.org). For peptide identification, MS/MS spectra were searched against a sequence database for the UniProt human reference proteome, including isoforms, with a set of common laboratory contaminant proteins appended (2017: 65,068 entries, or 2014: 59,079 entries) as indicated in Table S5. Search parameters included: ESI-QEXACTIVE-HCD scoring parameters, trypsin enzyme specificity with a maximum of two missed cleavages, 40% minimum matched peak intensity, ±20 ppm precursor mass tolerance, ±20 ppm product mass tolerance. Carbamidomethylation of cysteines and iTRAQ4 or TMT10 full labeling of lysines and peptide n-termini were set as fixed modifications. Allowed variable modifications were oxidation of methionine (M), acetyl (ProtN-term), and deamidated (N), with a precursor MH+ shift range of -18 to 64 Da. Identities interpreted for individual spectra were automatically designated as valid by optimizing score and delta rank1-rank2 score thresholds separately for each precursor charge state in each LC-MS/MS while allowing a maximum target-decoy-based false discovery rate (FDR) of 1.0% at the spectrum level. Identified peptides were organized into protein groups and subgroups (isoforms and family members) with Spectrum Mill's subgroup specific option enabled, so that peptides shared between subgroups are ignored for quantitation. TMT10 reporter ion intensities were corrected for isotopic impurities using Spectrum Mill's afRICA correction method and correction factors obtained from the reagent manufacturer's certificate of analysis. For quantitation at the peptide spectrum match level, $\log_2$ fold change (FC) reporter ion intensity ratios were calculated for each IP replicate. To obtain protein-level $\log_2$ FC values between index protein vs. control for each IP replicate, the median ratio was calculated from all peptide spectrum matches of subgroup specific peptides assigned to each protein subgroup.

Genoppi analysis

For each IP-MS experiment, starting with the protein-level quantification report generated by Spectrum Mill, we applied median normalization to protein $\log_2$ FC values between index protein vs. control IPs for each replicate, and then performed downstream analyses using Genoppi[24] (v1.0). Additional data

processing was performed for two experiments pre-Genoppi: for 'CACNA1C_wk7' the $\log_2$ FC values for one replicate was right-shifted by a small value (0.005) to facilitate direct comparisons with all other volcano plots without changing the results; for 'TCF4_wk1' additional contaminant proteins found in the CRAPome[73] database were removed. The Genoppi analyses include: i] calculating Pearson's correlation of $\log_2$ FC values between IP replicates, ii] calculating average $\log_2$ FC, and corresponding P-value and FDR, for each protein across IP replicates using a two-tailed one-sample moderated t-test from the limma[74] R package, iii] identifying statistically significant ($\log_2$ FC > 0 and FDR $\leq$0.1) index protein interactors (i.e., proteins with significantly higher abundance in the index protein IPs compared to the controls), iv] defining other non-significant ($\log_2$ FC $\leq$ 0 or FDR >0.1) proteins to be the 'non-interactors' (to serve as proxy for background proteome in enrichment analyses), and v] assessing overlap enrichment between the identified interactors and known interactors from InWeb[25] (compared to the non-interactors) using a one-tailed hypergeometric test. We performed quality control of each IP-MS experiment using two criteria: i] the $\log_2$ FC correlation between replicates must be >0.5, and ii] the index protein itself must be significant ($\log_2$ FC > 0 and FDR $\leq$0.1). Experiments that failed to meet these criteria were excluded from further analysis; those that passed QC are summarized in Table S5, with their analysis results provided in Table S6.

Co-expression analysis

We assessed pairwise co-expression between each index gene and all other protein-coding genes using data from four independent studies, including: i] Stickels et al.[29]: spatial transcriptomics in mouse neocortex (Puck_190921_19.digital_expression.txt.gz retrieved from: https://singlecell.broadinstitute.org/single_cell/study/SCP815/highly-sensitive-spatial-transcriptomics-at-near-cellular-resolution-with-slide-seqv2#study-download), ii] Maynard et al.[28]: spatial transcriptomics in human dorsolateral prefrontal cortex (count matrix retrieved from spatialLIBD R package: https://github.com/LieberInstitute/HumanPilot), iii] Velmeshev et al.[30]: single-cell RNA-seq in human cortex (rawMatrix.zip retrieved from: https://cells.ucsc.edu/?ds=autism), and iv] BrainSpan: bulk RNA-seq across human brain regions and developmental stages ("RNA-Seq Gencode v10 summarized to genes" dataset retrieved from: https://www.brainspan.org/static/download.html). We used two different methods for estimating co-expression to account for different statistical properties in these datasets. For the spatial transcriptomic datasets with very sparse gene expression matrices, we reasoned that the binary presence/absence of genes across physical locations would be the most informative, and therefore performed one-tailed Fisher's exact tests to calculate the significance of co-occurrence for each gene pair across locations. For the single-cell RNA-seq and BrainSpan datasets, we calculated a proportionality metric, ρ, for each gene pair using the propr R package[58] (v4.2.6); this metric is analogous to conventional correlation measures but has been shown to be better at capturing functional associations between genes in RNA-seq data.[75] After calculating either the Fisher's exact P-values or the proportionality ρ values for all gene pairs involving each index gene, we then performed rank-based inverse normal transformation to convert the values into co-expression Z-scores (where a positive score indicates that a gene has higher than average co-expression with the index gene compared to the rest of the genome).

We performed two-tailed Wilcoxon rank-sum tests to assess if the co-expression Z-scores between index genes and their interactors are significantly different from the scores between the index genes and other gene groups including: i] non-interactors detected in IP-MS, ii] known interactors from InWeb, and iii] all protein-coding genes.

Consolidating IP-MS datasets into interaction networks

We consolidated IP-MS datasets for the same index proteins into index-protein-specific networks; datasets derived from the same time points into time point-specific networks; and all datasets into an all combined network. For each network, we defined 'interactors' as proteins that show up as significant interactors in $\geq$1 source IPs contributing to the network, and the matching 'non-interactors' as proteins that show up as non-interactors in $\geq$1 source IPs but never as interactors in these IPs. In addition, we defined 'stringent interactors' as interactors that never show up as non-interactors in the source IPs. Finally, we removed proteins whose HGNC gene symbols could not be mapped to Ensembl[76] (GRCh37.p13) genomic positions and the index proteins for the source IPs from all 3 lists. The exclusion of index proteins ensured that enrichment signals in downstream analyses could not be driven by the index proteins themselves. Table S9 lists the interactors, non-interactors, and stringent interactors associated with each network.

SynGO gene set analysis

SynGO analysis of interactor genes in the all combined network was performed using the SynGO web browser[31] (dataset version: 20210225; https://syngoportal.org). The SynGO 'Biological Processes' annotations and the 'brain expressed' background set were used in the analysis.

Common variant enrichment analysis using MAGMA

To perform common variant risk enrichment analysis for each interaction network using MAGMA[32] (v1.09b), PGC GWAS summary statistics (https://www.med.unc.edu/pgc/download-results/) were obtained for schizophrenia (33,640 cases and 43,456 controls of EUR ancestry[3]; 22,778 cases and 35,362 controls of EAS ancestry[8]), ADHD (19,099 cases and 34,194 controls of EUR ancestry[33]), ASD (18,382 cases and 27,969 controls of EUR ancestry[34]), BIP (41,917 cases and 371,549 controls of EUR ancestry[35]), and MDD (170,756 cases and 329,443 controls of EUR ancestry[36]). GWAS summary statistics for height were obtained from the Neale Lab UK Biobank GWAS (round 2; 361,194 individuals of EUR ancestry[37]; https://www.nealelab.is/uk-biobank/) and Biobank Japan (159,095 individuals of EAS ancestry[38]; http://jenger.riken.jp/en/result). For each GWAS dataset, we first annotated variants to genes using the Human reference genome (GRCh37/hg19) with a flanking gene region of $\pm$250kb. Variants on sex chromosomes, with minor allele frequency (MAF) $\leq$ 0.05 in the study, or within the MHC region (chr6:22.5M-33.5M) were excluded from analysis. Next, gene-based P-values were computed using the SNP-wise Mean model in MAGMA. LD was estimated from the 1000 Genomes Project[77] phase 3 EUR or EAS panel to match the ancestry of each study. Competitive tests were used for gene-set comparison analysis between stringent interactors and non-interactors in each interaction network. Specifically, a linear regression model was built by MAGMA to test if genes within the interactor gene-set are more strongly associated with the phenotype of interest compared to the non-interactor gene-set. Inverse-variance weighted fixed-effect meta-analysis[78] was used to combine results across EUR and EAS ancestries for schizophrenia and height, and a one-tailed P-value was calculated from the meta-analyzed Z-score.

Common variant enrichment analysis using the GRS method

To complement the MAGMA analysis, we used an alternative genetic risk score (GRS) method and individual-level genotypes from the schizophrenia GWAS study cohorts (24,764 cases and 30,655 controls of EUR ancestry; 8,960 cases and 8,284 controls of EAS ancestry) to assess genetic risk enrichment in the interaction networks. IRB approvals for accessing the individual-level data were obtained from the PGC and Stanley Global Asia Initiatives (Data S1-S3). For each study cohort, we removed variants in the MHC region and variants with MAF $\leq$0.05 or low imputation quality (INFO $\leq$0.8), and then mapped the remaining variants to the stringent interactors or non-interactors associated with each network with a flanking gene region of $\pm$250kb. Next, we used PLINK[59] (v1.9) and the in-sample LD to clump variants within the interactor or non-interactor gene-sets into independent association signals. The clumping was performed with a window of 250kb, R^2> 0.2, and a P-value threshold of 1. The out-of-sample GRS for each individual and each gene-set was then calculated as $\sum \log(OR) * G$, in which OR is the estimated odds ratio from the leave-one-out GWAS meta-analysis for the clumped index variants within the gene-set and G is the genotype dosage. To test if the stringent interactors in a network contribute more genetic risk compared to the non-interactors, we fit a linear regression model: $GRS_{ij} = P_i + I_j + P_i * I_j + Cov_i$, where i and j denote individual index and gene index, respectively, P is the case/control status, I is interactor/non-interactor status, $P*I$ is an interaction term, and Cov includes 10 genetic principal components. We tested whether the $P*I$ interaction term is significantly larger than zero, which captures whether the difference of GRS between cases and controls calculated in the interactor gene-set is significantly larger than the non-interactor gene-set. Inverse-variance weighted fixed-effect meta-analysis was used to combine the test statistics for the interaction term across study cohorts and ancestries, and a one-tailed P-value was calculated from the meta-analyzed Z-score. Finally, as a negative control, we performed an analogous GRS analysis for height; in this case, the GRS was calculated as $\sum \log(beta) * G$, where $beta$ is the effect size estimate from the EUR or EAS height GWAS for clumped index variants.

Rare variant enrichment analysis

Gene-based association statistics derived from exome sequencing data were obtained for schizophrenia (P-values in 'P meta' column from Table S5 of Singh et al.[9]), ASD (Q-values in 'qval_dnccPTV' column from Table S2 of Satterstrom et al.[40]), and DD (P-values in 'denovoWEST_p_full' column from Table S2 of Kaplanis et al.[41]). For each phenotype and each network, a one-tailed KS test was used to test whether

the stringent interactors in the network have more significant association scores (i.e., smaller P-values or Q-values) compared to the non-interactors.

Transcriptional perturbation enrichment analysis

Differentially expressed genes (DEGs) between schizophrenia patients vs. controls identified in 20 prefrontal cortex cell types were retrieved from Table S6 of Ruzicka et al.[17] The up- and down-regulated DEGs were analyzed as a joint set in the primary analysis, and then as separate sets in the secondary follow-up analyses. One-tailed P-values were calculated using a hypergeometric distribution to assess the overlap enrichment between interactors in our networks and the cell-type-specific DEGs. For each hypergeometric test, the 'population' was defined as all stringent interactor or non-interactor genes associated with a network and 'success in population' was defined as the stringent interactors in the network. The 'sample' contained DEGs in a celltype that were found in the population and 'success in sample' was the overlap between the interactors and the DEGs.

Social Manhattan plot

Genes mapped to 287 genome-wide significant regions in the combined discovery-replication meta-analysis of the PGC schizophrenia GWAS (phase 3) were retrieved from Table S3 of the paper.[10] We excluded non-coding genes and genes in the MHC region, and obtained the genomic positions of the remaining genes from Ensembl[76] (GRCh37.p13). We additionally included *SYNGAP1* by mapping it to the only MHC region SNP (rs140365013) included in the GWAS meta-analysis. Next, we intersected these GWAS genes with our PPI data to identify the subset of GWAS genes that are either an index gene or an interactor of an index gene. We generated a Manhattan plot for these genes using the GWAS P-values of their associated index SNPs and plotted links between the genes to indicate observed interactions in our 3. In addition, we retrieved the list of GWAS genes prioritized by FINEMAP or SMR analysis from Table S12 of the PGC paper and highlighted their overlap with genes prioritized by our data in the plot. For ease of visualization, GWAS P-values were capped at $P = 1e\text{-}25$ and genes in the PCDHA@ gene cluster were collapsed into one gene in the plot.

HCN1 network drug target query

To identify existing drugs targeting genes in the combined HCN1 network, we performed a batch query using the Open Targets Platform[79] (https://platform.opentargets.org). For each resulting drug-target entry, the corresponding drug mechanism information was retrieved from ChEMBL[80] (https://www.ebi.ac.uk/chembl/g/#browse/mechanisms_of_action).